Progress in Uranium Chemistry: Driving Advances in Front-End Nuclear Fuel Cycle Forensics

Kevin J. Pastoor, R. Scott Kemp, Mark P. Jensen, Jenifer C. Shafer

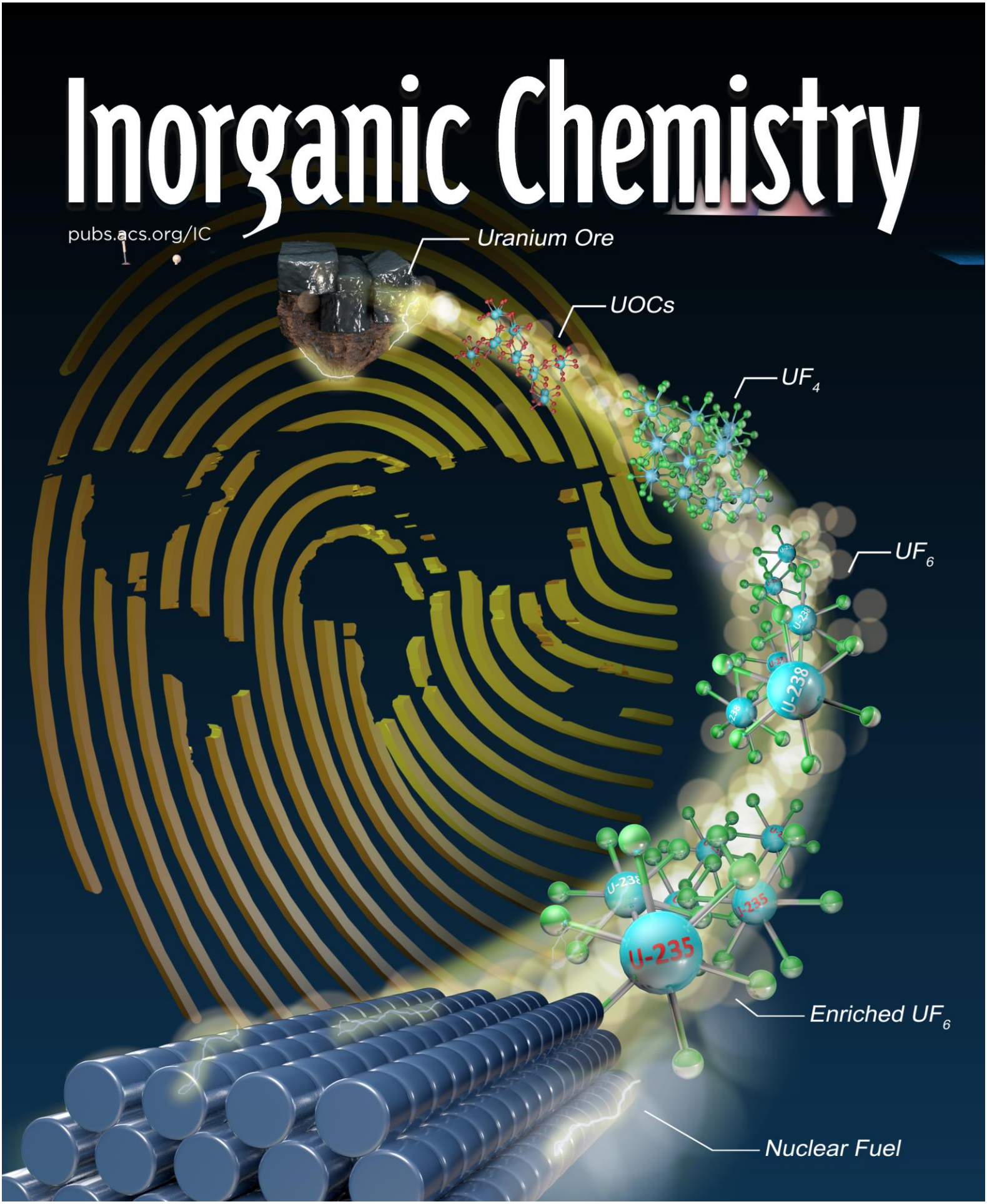
Inorganic Chemistry
pubs.acs.org/IC
Uranium Ore
UOCs
UF4
UF6
U-238
U-235
Enriched UF6
Nuclear Fuel

Inorganic Chemistry

pubs.acs.org/IC Viewpoint

Progress in Uranium Chemistry: Driving Advances in Front-End Nuclear Fuel Cycle Forensics

Kevin J. Pastoor, R. Scott Kemp, Mark P. Jensen, and Jenifer C. Shafer*

Cite This: https://doi.org/10.1021/acs.inorgchem.0c03390 Read Online

ACCESS | Metrics & More | Article Recommendations

ABSTRACT: The front-end of the nuclear fuel cycle encompasses several chemical and physical processes used to acquire and prepare uranium for use in a nuclear reactor. These same processes can also be used for weapons or nefarious purposes, necessitating the need for technical means to help detect, investigate, and prevent the nefarious use of nuclear material and nuclear fuel cycle technology. Over the past decade, a significant research effort has investigated uranium compounds associated with the front-end of the nuclear fuel cycle, including uranium ore concentrates (UOCs), UF_4, UF_6, and UO_2F_2. These efforts have furthered uranium chemistry with an aim to expand and improve the field of nuclear forensics. Focus has been given to the morphology of various uranium compounds, trace elemental and chemical impurities in process samples of uranium compounds, the degradation of uranium compounds, particularly under environmental conditions, and the development of improved or new techniques for analysis of uranium compounds. Overall, this research effort has identified relevant chemical and physical characteristics of uranium compounds that can be used to help discern the origin, process history, and postproduction history for a sample of uranium material. This effort has also identified analytical techniques that could be brought to bear for nuclear forensics purposes. Continued research into these uranium compounds should yield additional relevant chemical and physical characteristics and analytical approaches to further advance front-end nuclear fuel cycle forensics capabilities.

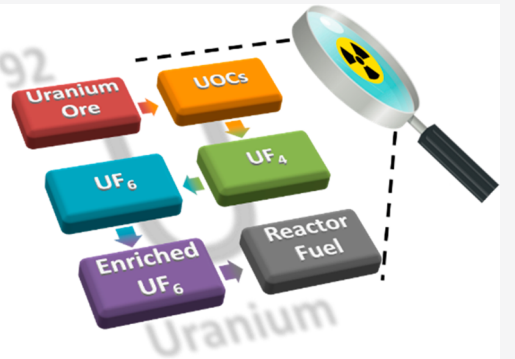

INTRODUCTION

The front-end of the nuclear fuel cycle is comprised of the chemical and physical processes necessary to extract uranium from the earth and prepare it for use in a nuclear reactor. These processes are mining, milling, conversion, enrichment, and fuel fabrication.[1] The same set of processes can also be used to prepare uranium suitable for use in a nuclear weapon. This dual-use nature of nuclear fuel cycle technology has propelled international agreements and the development of technical means aimed toward detecting, investigating, and preventing the nefarious use of nuclear technology and nuclear materials. One of the technical means is the field of nuclear forensic science, which provides insight into nuclear or radioactive materials found outside regulatory control.[2] Nuclear forensics relies heavily on analytical and inorganic chemistry to identify, measure, and understand chemical and physical signatures and indicators that are created or destroyed in the material during production, storage, and use.[3−6] These signatures and indicators can be interpreted to help ascertain a material's identity, origin, and history and suggest its intended use. The term nuclear forensics has traditionally been used in the context of nuclear security, specifically the analysis of illicitly trafficked material, but the same capabilities are also applicable to nuclear nonproliferation efforts, such as the investigation of undeclared nuclear activities.[7] For the purpose of this paper, the term nuclear forensics is considered in this broader context including matters of nuclear security and nuclear nonproliferation. Because of its role within nuclear security and nonproliferation efforts, there is a need to continuously advance nuclear forensics.[4,8−10] One avenue for achieving this aim is furthering the chemistry of uranium compounds found within the front-end of the nuclear fuel cycle. Before proceeding, it is important to highlight certain terminology encountered within the nuclear forensics community, specifically the terms upstream and downstream as they relate to the nuclear fuel cycle. In the context of nuclear forensics, upstream refers to activity before enrichment and downstream refers to activity following enrichment.

There are several key uranium compounds within the front-end of the nuclear fuel cycle (Figure 1). The first uranium compounds encountered, in the mining process, are uranium minerals that comprise uranium ore deposits. Currently, the

Received: November 16, 2020

https://doi.org/10.1021/acs.inorgchem.0c03390
Inorg. Chem. XXXX, XXX, XXX−XXX

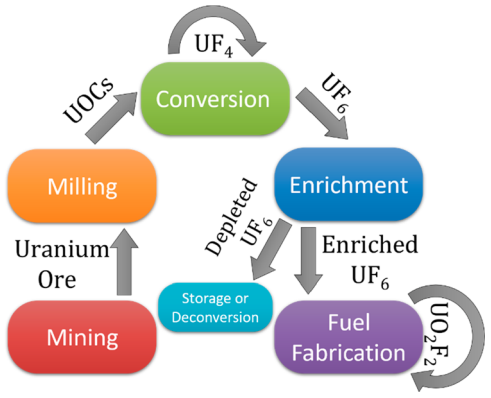

Figure 1. Front-end of the nuclear fuel cycle and key uranium compounds associated with each process.

International Mineralogical Association recognizes 217 mineral species containing uranium as an essential structural constituent; excluding metalloids and nonmetals, uranium ranks 11th among elements with the greatest number of mineral species.[11,12] Given the breadth of the subject and other available sources, uranium ores and uranium mineralogy will not be discussed further in this paper. After mining, uranium ore is milled using physical and chemical processes to separate uranium from the other constituents.[13,14] The resulting product is known as uranium ore concentrates (UOCs), often is referred to as yellowcake. The term UOCs encompasses several key uranium compounds including UO_2, UO_3, U_3O_8, and $UO_2(O_2)\cdot xH_2O$ (where x = 2 or 4). An alternative, widely used, method to produce UOCs is known as in situ leaching (ISL). ISL mining of uranium effectively combines mining and milling into a single operation, extracting uranium from an ore body in solution rather than removing pieces of the ore body from the ground and then separating and purifying the uranium to produce UOCs. Following production of UOCs, the next process in the nuclear fuel cycle, conversion, transforms UOCs into uranium hexafluoride (UF_6), which is suitable for use in the enrichment process because of its high vapor pressure, ease of sublimation, and the fact that fluorine has only one natural isotope.[15,16] In addition to UF_6, the conversion process produces another key uranium compound, uranium tetrafluoride (UF_4), an intermediate within the process. Following conversion, UF_6 is altered isotopically via enrichment, for which the two most common technologies are gaseous diffusion and gaseous centrifugation. This results in enriched and depleted UF_6 streams, where enriched UF_6 possesses a ^{235}U concentration of >0.711 wt % and depleted UF_6 a ^{235}U concentration of <0.711 wt %.[16,17] Last, during fuel fabrication, UF_6 is typically converted to UO_2 or uranium metal and prepared for use in a nuclear reactor.[18,19] Depending on the process used, one of several intermediate uranium compounds may be formed including uranyl fluoride (UO_2F_2), ammonium diuranate (ADU), or ammonium uranyl carbonate (AUC). Using a process similar to fuel fabrication, depleted UF_6 is sometimes converted to a more stable uranium oxide, in a process referred to as deconversion, for storage as very low-level waste. Among the possible intermediate uranium compounds encountered during fuel fabrication or UF_6 deconversion, UO_2F_2 is particularly noteworthy because it results from hydrolysis of UF_6. Thus, UO_2F_2 is significant from a nuclear forensics perspective because it is formed from UF_6 releases from process equipment or a storage cylinder into the environment.

Over the past decade, a significant research effort has focused on several of these key uranium compounds with the aim of advancing the science of these compounds and the field of nuclear forensics. In particular, recent research has examined the morphology of various uranium oxides, with a focus on discerning process history or process conditions for a particular sample of material.[20−32,46] One outcome of these efforts was a lexicon to standardize descriptions of material images for nuclear forensics, indicating a likely increasing role for morphology within nuclear forensics.[33] Recent research has also investigated elemental and chemical impurities present in process samples of uranium compounds, also with a focus of discerning process history as well as the origin of the uranium.[34−42,44,45,47−49] For example, the concentrations of rare-earth elements (REEs) have been found to be potentially useful for identifying the origin of UOCs.[41] Other research has focused on understanding the degradation of uranium compounds, particularly under environmental conditions.[51−69] These efforts are important for nuclear forensics investigations of aged materials or samples exposed to the environment. For instance, various UOCs stored in controlled relative humidity (RH) and temperature conditions have undergone chemical reactions, converting them to different uranium compounds.[51,56−58] One final focus area has been developing improved or new analytical techniques for probing various key uranium compounds.[70−76] For example, laser-induced breakdown spectroscopy (LIBS), which can be packaged in a field-deployable form factor, has been studied as a possible technique to rapidly identify various uranium oxides and UO_2F_2.[70,74] Overall, the significance of the recent research and the growing importance of nuclear forensics is evident in the proposal and establishment of Nuclear Proliferomics, a field of study focused on building comprehensive databases of nuclear materials' properties that could be leveraged through various data analytics and machine-learning techniques to advance nuclear forensics analyses.[77]

This work will cover, in brief, these recent research efforts as they apply to three categories of key uranium compounds within the front-end of the nuclear fuel cycle: UOCs, uranium fluorides (UF_4 and UF_6), and UO_2F_2. Overall, there remains a lack of understanding regarding some of the fundamental inorganic chemistry that drives the creation or destruction of the chemical and physical signatures observed in these uranium compounds. For example, understanding how various process conditions affect the levels of impurities throughout the nuclear fuel cycle, how the crystallinity of these compounds changes in response to varying process conditions, or how exposure to environmental conditions drives changes in chemical speciation. The existing gaps are the impetus behind this paper, to raise awareness of research opportunities that may continue to advance uranium chemistry and, by extension, the field of nuclear forensics.

UOCS

Among the key uranium compounds associated with the front-end of the nuclear fuel cycle, UOCs have received the greatest focus of recent nuclear-forensics-related research. One significant reason for this focus is the ubiquity of UOCs and their ease of transportation, which makes them attractive for illicit trafficking and thus an ideal target for signature development.[43] Recent research has primarily focused on

https://doi.org/10.1021/acs.inorgchem.0c03390
Inorg. Chem. XXXX, XXX, XXX−XXX

developing signatures to identify the origin, process history, and postproduction history of UOCs by investigating several aspects of UOCs including the morphology, trace element composition, and environmental degradation, as well as developing new or improved techniques for analyzing UOCs.

UOC Morphological Studies. Several recent studies have investigated morphological features of UOCs, primarily accessed via scanning electron microscopy (SEM), as a possible nuclear forensics signature for determining aspects of the material's process history and postproduction history. With respect to process history, studies have been conducted to determine whether morphological features can be leveraged to identify the precursors used to produce a particular UOC, for example, was a sample of U_3O_8 made by calcining uranyl peroxide [$UO_2(O_2)\cdot xH_2O$] or a diuranate compound. In addition to precursors, morphological studies have also considered the effect of process conditions, such as the calcining temperature, on the resulting product's morphology. Last, morphological features have also been studied in connection with the degradation or aging of UOCs under various environmental conditions.

Manna et al. studied the morphology of ADU [$(NH_4)_2U_2O_7$] and the resulting morphology of uranium oxides produced via calcination of ADU at various temperatures, 450, 550, 650, and 750 °C.[31,32] At lower magnifications, the uranium oxides they produced possessed a morphology similar to that of the starting ADU material, indicating that the morphology of the ADU was retained through the calcination process. Increased magnification revealed the formation of pores in the uranium oxides produced at 550 °C and higher temperatures. The pores likely resulted from the release of gaseous NH_3 and H_2O during calcination. They also observed that the uranium oxide surface area increased with respect to calcination temperatures up to 550 °C, but further increases in the calcination temperature resulted in a decrease in the surface area. Later, Tamasi et al. investigated the morphology of $UO_2(O_2)\cdot xH_2O$ and the resulting morphology of uranium oxides (UO_2, α-U_3O_8, and α-UO_3) produced from $UO_2(O_2)\cdot xH_2O$.[30] Both α-UO_3 and α-U_3O_8 were prepared by calcining $UO_2(O_2)\cdot xH_2O$ at 400 and 800 °C, respectively, and UO_2 was prepared by a two-step process, calcination at 400 °C followed by high temperature (500 °C) reduction under H_2. All of the materials that they analyzed were described, according to an established lexicon, as clumped agglomerates comprised of rounded and subrounded particles.[33] They also observed that the various uranium oxides possessed an overall morphology similar to that of the uranyl peroxide precursor, indicating that the overall morphology was preserved through calcination and reduction. Overall, these studies indicated that morphological features could potentially serve as an indicator for some aspects of UOC process history. Specifically, these studies suggested that the morphology may be able to identify the precursor material and process conditions used to prepare a given UOC material.

Building significantly on this potential, several recent studies investigated the morphology of various UOCs using a software program, morphological analysis for materials (*MAMA*), to quantitatively characterize the particles from SEM images.[20−22,25−28] Olsen et al. studied the differences in the morphological features of U_3O_8 materials produced by calcining α-UO_3 at various temperatures, 600, 650, 700, 750, and 800 °C.[25] While they did observe some qualitative variations among the U_3O_8 samples produced at the various calcining temperatures, processing the SEM images through the *MAMA* particle segmentation software enabled a quantitative determination of the morphological statistics for the material. From the available morphological attributes, it was determined that microparticle size distributions and particle circularity were able to statistically differentiate between the various U_3O_8 samples (Figure 2). Schwerdt et al. examined the morphology of several different samples of UO_3 prepared by calcining a uranyl peroxide [$UO_2(O_2)\cdot 2H_2O$], known as metastudtite, at various temperatures, 250, 300, 350, 400, and 450 °C.[28] Qualitatively, the most significant difference observed among the various UO_3 samples was the tendency of microparticles to fracture at higher calcination temperatures. Otherwise, qualitative analysis showed that the morphologies of the $UO_2(O_2)\cdot 2H_2O$ and UO_3 samples were quite similar. Quantifying the morphological features using the *MAMA* software showed that the particle size distribution decreases and the particle circularity increases as the calcination temperature is increased from 250 to 400 °C. They combined their data with the earlier results from Olsen et al. to examine the trends in the particle size and shape over a larger temperature range. In general, the particle size distribution decreases as the calcination temperature is increased from 250 to 400 °C, reaches a minimum between 400 and 600 °C, and increases as the temperature is increased from 600 to 800 °C.[25,28] On the other hand, the particle circularity continually increases as the calcination temperature is increased from 250 to 800 °C. Overall, these studies demonstrate that quantifying the morphological features of

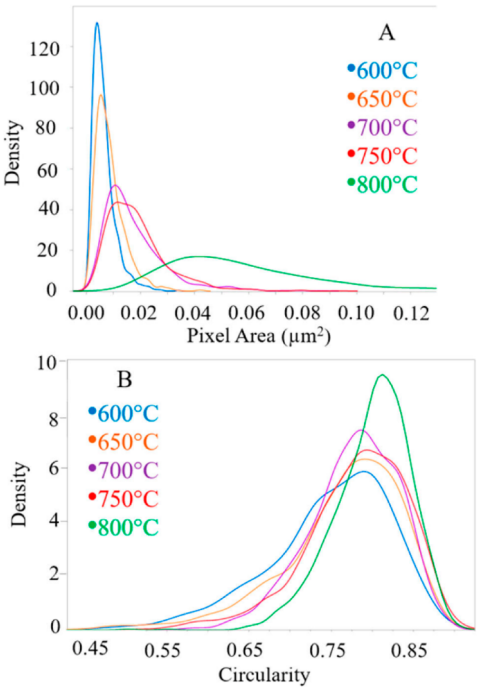

Figure 2. Density plots of the microparticle area (A) and circularity (B) for U_3O_8 samples prepared by calcining α-UO_3 at various temperatures. In general, both the microparticle area and circularity increase as the calcination temperature is increased. The density plots were generated via quantification of the morphological features from SEM images using the *MAMA* software. Reprinted with permission from ref 25. Copyright 2017 American Chemical Society.

https://doi.org/10.1021/acs.inorgchem.0c03390
Inorg. Chem. XXXX, XXX, XXX−XXX

UOCs could potentially be used to distinguish between the UOC materials produced by various process conditions.

Two studies using the *MAMA* software investigated the potential to discern different precursors used to prepare UOCs. Abbott et al. studied UO_2 prepared by H_2 reduction of three different uranium oxide precursors, *am*-UO_3, α-UO_3, and α-U_3O_8.[20] They observed that the morphology for each UO_2 material was qualitatively distinct from one another and the morphology of each UO_2 material was qualitatively similar to that of the uranium oxide from which it was prepared. The UO_2 prepared from α-UO_3 was significantly distinct from the other UO_2 samples, and thus additional analysis was not performed. Quantifying the morphological features of the remaining UO_2 samples confirmed their qualitative observations; that is, quantification showed similar particle areas, and no statistical difference in circularity, between the starting uranium oxides, *am*-UO_3 and U_3O_8, and their respective UO_2 product. Morphological quantification also statistically differentiated between the two UO_2 samples, indicating that the UO_2 prepared from *am*-UO_3 was smaller in size and less circular than the UO_2 prepared from U_3O_8. Thus, this study demonstrated the utility of quantitative morphological analysis to differentiate UO_2 materials prepared from different uranium oxide precursors.

Schwerdt et al. conducted a significantly expanded investigation of UOCs prepared from different uranium precursors.[27] Specifically, they investigated samples of UO_3, U_3O_8, and UO_2 prepared from ADU, uranyl peroxide, sodium diuranate (SDU, $Na_2U_2O_7$), AUC [$UO_2CO_3{\cdot}2(NH_4)_2CO_3$], and uranyl hydroxide [UH, $UO_2(OH)_2$]. The UH was prepared by reacting MgO with uranyl nitrate; the resulting product is often referred to as magnesium diuranate (MDU) but is known to be uranyl hydroxide hydrates. The morphologies of nearly all of the starting uranium compounds were qualitatively distinct; the exceptions were ADU and SDU, which possessed qualitatively similar morphologies. The morphologies of the UO_3 samples produced by calcining the various starting compounds at 400 °C remained qualitatively distinct from one another; however, the higher calcination temperature, 800 °C, used to produce U_3O_8 resulted in samples with qualitatively less distinct morphologies. To overcome this limitation, the *MAMA* software was used to quantify the morphologies of the UO_3, U_3O_8, and UO_2 samples, specifically, the size or area of the particles and ellipse aspect ratio, a ratio of the length and width for an ellipse fitted to the particle. For the UO_3 samples, the particle sizes were statistically different, apart from the UO_3 produced from ADU and SDU. However, by adding the ellipse aspect ratio, all UO_3 samples could be statistically differentiated from each other (Figure 3). For the U_3O_8 materials, both the particle sizes and ellipse aspect ratio were statistically different for each synthetic pathway. Last, for the UO_2 materials, the particle sizes were statistically different, except for the UO_2 produced from SDU and ADU and the UO_2 produced from AUC and UH. Again, by adding the ellipse aspect ratio, all of the UO_2 samples could be statistically differentiated from each other.

More recently, Nizinski et al. investigated the effects of process history on the morphology of UOCs prepared from uranium ore.[46] They prepared UOC samples using two different commercial solvent extraction processes: the Dapex process and the Amex process. Following solvent extraction, the uranium was precipitated as ADU and calcined to form UOCs that were a mixture of UO_3 and U_3O_8. Qualitatively, the morphologies of the UOCs produced by either solvent extraction process were remarkably similar; the primary difference was that the UOCs produced via the Amex route appeared more densely agglomerated. However, using the *MAMA* software to quantify the particle sizes and shapes of the samples, they were able to statistically differentiate between the UOCs produced by the different solvent extraction processes. Overall, these studies demonstrate the utility of quantitative morphological analysis to differentiate between various UOC samples, especially those that appear qualitatively similar. Additionally, these studies demonstrate that quantitative morphological analysis could potentially be used to discern the production pathway for several key uranium oxide UOCs.

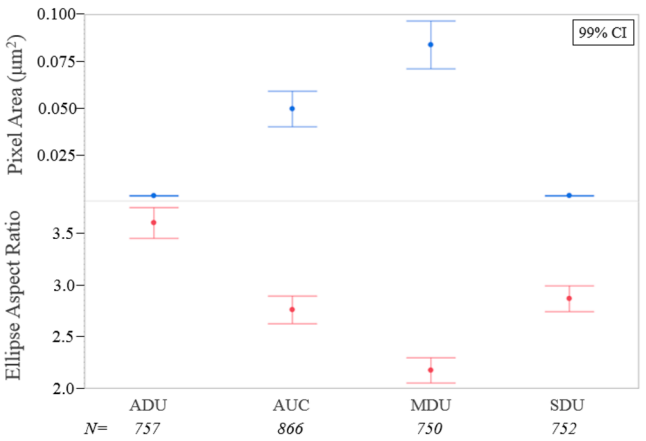

Figure 3. Quantified morphological features, pixel area (top) and ellipse aspect ratio (bottom), of the UO_3 samples produced by calcining ADU, AUC, MDU (UH), and SDU at 400 °C for 8 h. All UO_3 samples could be differentiated from one another by combining the results for both morphological features. Reprinted with permission from ref 27. Copyright 2019 De Gruyter.

Finally, a recent study investigated the morphological changes caused by aging UOCs under various environmental conditions. Tamasi et al. studied three U_3O_8 samples, one pure α-U_3O_8 and two impure U_3O_8 samples, aged for 2 years in four different conditions, cool and dry (5 °C, 25% RH), cool and humid (5 °C, 97% RH), warm and dry (37 °C, 15% RH), and warm and humid (37 °C, 89% RH).[29] Using SEM, the morphologies of the samples were qualitatively characterized to identify changes caused by exposure to the various temperature and humidity conditions. For the pure α-U_3O_8 stored under the lower humidity conditions, there were no apparent changes to its morphology, but storage under higher humidity conditions resulted in an eroded or dissolved surface appearance. The particle size for the sample stored in warm and humid conditions also increased, likely the result of water absorption. For the two impure U_3O_8 samples, changes in the morphology were observed for all storage conditions, and similar to the pure α-U_3O_8 sample, the greatest changes were observed for the samples stored in humid conditions. These results indicate that environmental exposure can induce morphological changes in U_3O_8, and impurities present in U_3O_8 may enable more significant morphological changes in samples exposed to various environmental conditions. Morphological changes resulting from environmental exposure may be useful as an indicator for aspects of the postproduction history of UOCs; however, more studies, including other UOC chemical forms, will be required.

https://doi.org/10.1021/acs.inorgchem.0c03390
Inorg. Chem. XXXX, XXX, XXX−XXX

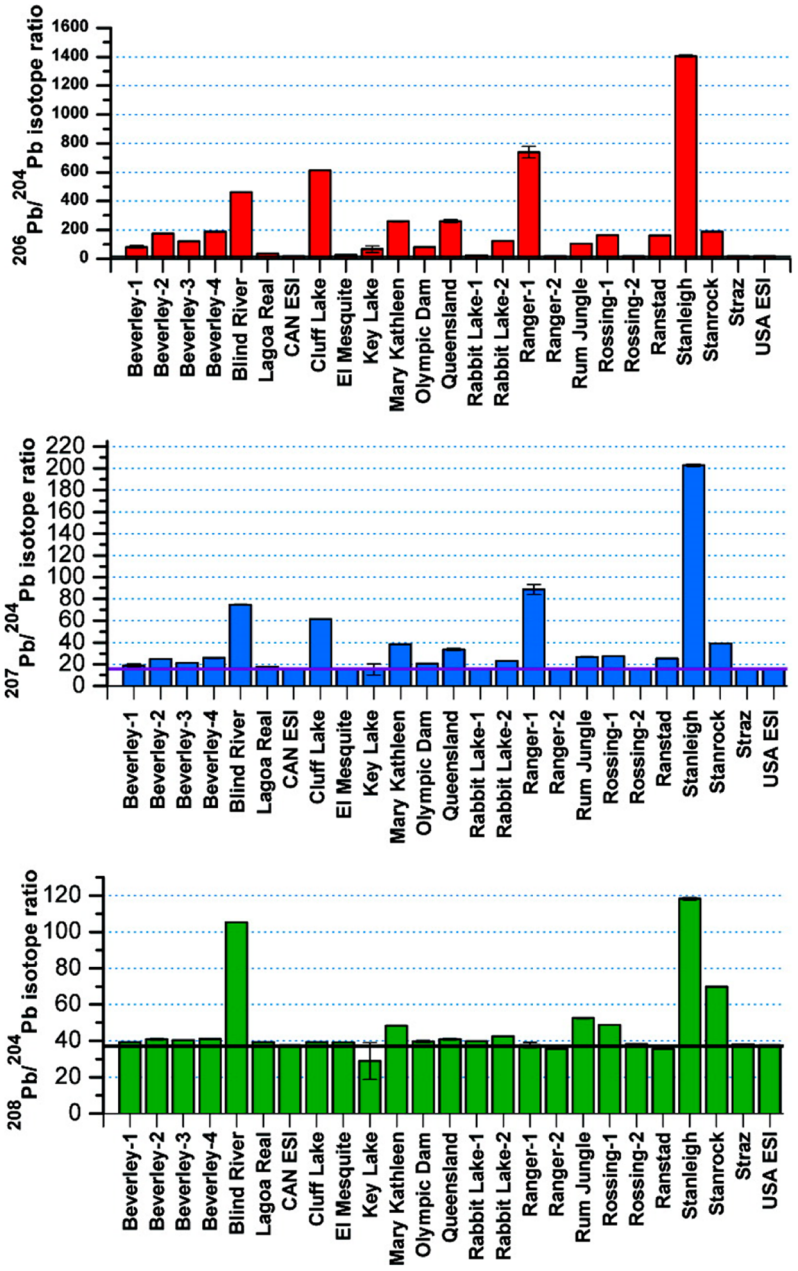

Figure 4. Lead isotopic ratios for various UOC samples. The current natural lead isotopic ratios are marked with a solid line. Reprinted with permission from ref 42. Copyright 2009 American Chemical Society.

Trace Elements in UOCs. A critical chemical signature for any uranium material, including UOCs, is the relative abundance of uranium isotopes that it contains. These elemental data, primarily determined using high-resolution mass spectrometry, provide key information as to whether the uranium is natural uranium (99.284 wt % ^{238}U, 0.711 wt % ^{235}U, and trace ^{234}U) or if it has been altered through either enrichment or nuclear reactions. Beyond the isotopics of uranium, recent research has investigated other elemental data that a uranium sample may contain. In particular, UOCs have been studied to determine whether trace elemental data could be leveraged to identify the origin and process history for UOCs.

The relative abundance of trace element isotopes, particularly lead, strontium, molybdenum, neodymium, and samarium isotopes, has been studied to investigate their utility in determining the origin of uranium. Svedkauskaite-LeGore et al. analyzed several uranium ore samples from two mines in Australia and eight UOCs from various origins.[39] Using multicollector inductively coupled plasma mass spectrometry (MC-ICP-MS), they determined the relative abundance of the four stable lead isotopes (^{204}Pb, ^{206}Pb, ^{207}Pb, and ^{208}Pb) in the samples. Three of the stable lead isotopes, ^{206}Pb, ^{207}Pb, and ^{208}Pb, are known as radiogenic lead; that is, they are produced from the radioactive decay of uranium and thorium. Thus, the abundances of radiogenic lead isotopes can vary throughout the earth's crust, particularly in locations where uranium and thorium are more or less abundant. Using the ratio of ^{207}Pb/^{206}Pb, they were able to differentiate between the uranium ore and UOC samples from nearly every different geographic origin. Exceptions were an Australian mine and a

https://doi.org/10.1021/acs.inorgchem.0c03390
Inorg. Chem. XXXX, XXX, XXX−XXX

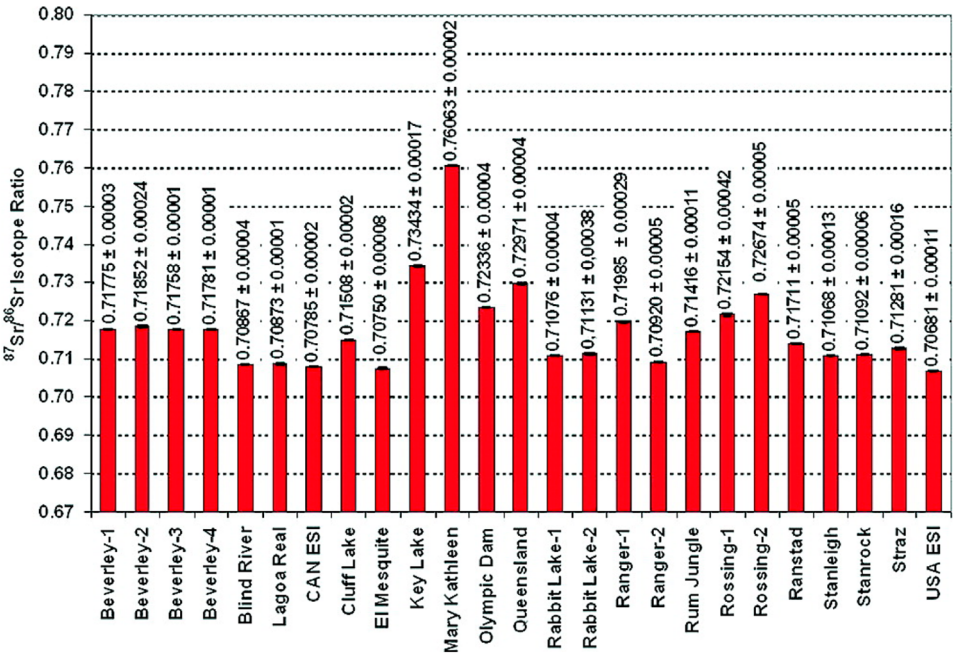

Figure 5. Strontium isotopic ratios for various UOC samples. Reprinted with permission from ref 42. Copyright 2009 American Chemical Society.

Namibian mine; the UOC samples from these locations possessed a similar $^{207}Pb/^{206}Pb$ ratio. Varga et al. also investigated trace element isotopes in UOCs, analyzing 25 samples from 19 different origins.[42] They primarily evaluated the ratios of radiogenic lead to primordial lead, that is, $^{206}Pb/^{204}Pb$, $^{207}Pb/^{204}Pb$, and $^{208}Pb/^{204}Pb$, and observed the variability in the ratios between the samples from different origins (Figure 4). However, they also observed the variability within a set of samples collected from the same origin, indicating a limitation to determining the origin of a sample based on lead isotopics alone. In addition to lead isotopics, they also determined the relative abundance of strontium isotopes in the samples. Using the ratio of $^{87}Sr/^{86}Sr$, they also observed the variability between the samples from different origins: the variation in the ratio of $^{87}Sr/^{86}Sr$ arises from β decay of long-lived ^{87}Rb to ^{87}Sr and the varying ratio of Rb/Sr in nature. Unlike the lead isotopics, they observed less variability in the ratio of $^{87}Sr/^{86}Sr$ for a set of samples from the same origin (Figure 5). Furthermore, combining both lead and strontium isotopic data increased the confidence in determining the geographic origin of a UOC sample.

Rolison et al. and Migeon et al. recently investigated the molybdenum isotope composition of UOCs. Rolison et al. used MC-ICP-MS to examine 31 UOCs from various geographic regions and 1 parent uranium ore associated with one of the UOCs.[48] They found that the ^{98}Mo composition among the UOCs varied with a range consistent with variations in the ^{98}Mo composition for natural materials. The variation in the ^{98}Mo composition for UOCs can arise from variations of ^{98}Mo in the parent uranium ore, fractionation of molybdenum isotopes during the production of UOCs, or contamination from a molybdenum source during production. While they were unable to assess the role of molybdenum contamination, the variation of ^{98}Mo in UOCs fell within the range observed for molybdenite minerals, indicating that variations of ^{98}Mo in the parent uranium ore is primarily responsible for the variations observed in UOCs. However, comparing the parent uranium ore with its corresponding UOC, they determined that fractionation occurred during production, resulting in a greater ^{98}Mo composition in the UOC. Thus, they concluded that both variation in the ^{98}Mo composition of uranium ore and fractionation during the production of UOCs contribute to the overall variation of ^{98}Mo in UOCs. Migeon et al. also investigated a set of UOCs using MC-ICP-MS.[49] They observed that UOCs produced from uranium ore of magmatic origin exhibited a different, higher ^{98}Mo composition compared to UOCs produced from uranium ores of sedimentary origin. They also observed that fractionation of molybdenum can occur during UOC production and noted that shifts in the ^{98}Mo composition during UOC production are likely affected by several factors of the production process, for example, the chemicals used and pH of the solutions. Their observations are consistent with the conclusion of Rolison et al. that the parent uranium ore is primarily responsible for ^{98}Mo variations in UOCs and that fractionation during UOC production will likely alter the ^{98}Mo composition relative to the parent uranium ore. However, the effect of specific UOC production conditions on the ^{98}Mo composition is not fully known at this time. Overall, the use of the molybdenum isotope composition, in combination with other trace elements or isotopic data, to help ascertain the origin of UOCs appears promising.

Krajko et al. developed a procedure to determine the ratio of $^{143}Nd/^{144}Nd$ in uranium materials.[50] They analyzed uranium ore samples from four origins as well as UOCs from 20 different origins. The $^{143}Nd/^{144}Nd$ ratios for the samples exhibited large variations and thus, they were able to distinguish most samples from one another. Variations in the ratio of $^{143}Nd/^{144}Nd$ arise from α decay of long-lived ^{147}Sm to ^{143}Nd and the varying ratio of Sm/Nd in nature. Additionally, they observed less variability for neodymium isotopics within a set of samples from the same origin compared to the variability observed for strontium or lead isotopics. Although not attempted in this study, combining neodymium isotopic data

https://doi.org/10.1021/acs.inorgchem.0c03390
Inorg. Chem. XXXX, XXX, XXX−XXX

with strontium and lead isotopic data could further improve the capability of distinguishing between UOCs from various geographic origins. More recently, Shollenberger et al. investigated samarium isotopes in UOCs as a possible means to determine the origin of uranium.[47] The potential utility of samarium isotopes arises from the large thermal neutron capture cross section of ^{149}Sm, meaning that there is a high probability that a free neutron present in a uranium ore body will be captured by ^{149}Sm, transmuting it to ^{150}Sm. Thus, variations in the thermal neutron activity and ages between different ore bodies could yield distinct ^{149}Sm and ^{150}Sm compositions. They analyzed 32 UOCs from different origins and were able to distinguish between approximately half of the samples based on their ^{149}Sm and ^{150}Sm compositions. The UOCs with resolved and anticorrelated samarium isotope compositions were typically produced from older uranium ore deposits containing higher concentrations of uranium. The ^{149}Sm and ^{150}Sm compositions of UOCs were indicative of the uranium ore's geologic origin and, combined with other isotopic signatures, could be used to help identify the origin of UOCs. Overall, the use of trace element isotopes to help determine the origin of uranium material appears to be promising; building a comprehensive database of isotopic data for UOCs produced around the globe would significantly improve the utility of this potential capability.

The relative abundance of lanthanides or REEs in UOCs has also been studied as a possible means to determine the origin of uranium. Varga et al. analyzed 38 UOCs from 31 different origins.[41] They found that the relative concentrations of REEs, also referred to as the REE pattern, varied significantly among the samples. As a standalone indicator, it may be useful in determining the origin of a material if compared to a database of known references. Without a reference, the REE pattern could only be used to help narrow the possible origins of a uranium material. By comparing their results with those reported for uranium minerals, they observed that the REE pattern found in ores is largely preserved through the uranium milling process. Keegan et al. also investigated the elemental impurities for several UOC samples.[44] Consistent with the findings of Varga et al., they determined that the REE patterns were distinctive for certain, but not all, ore deposit types and concluded that REE patterns could serve as a complementary, but not a standalone, indicator for the origin of UOCs.

Last, other trace elements and compounds have been investigated as possible means to determine the origin or process history of UOCs. Badaut et al. investigated the anionic impurities (i.e., fluoride, chloride, nitrate, sulfate, and phosphate) in 12 UOCs from 8 different origins.[45] They found significant variation between samples from different origins; however, they also observed variation between multiple samples from a single origin. Similar to other trace element investigations, they concluded that anionic impurities could be a complementary, but not standalone, indicator for the origin of UOCs. Later, Keegan et al. studied the impurities of 24 UOC samples and found that high concentrations of certain elements or compounds may indicate aspects of the uranium milling process chemistry used to produce the UOCs.[44] For example, they found high concentrations of calcium or magnesium in certain samples, suggesting the use of lime or MgO as a precipitant. Additionally, their results indicate that Cl^- and SO_4^{2-} impurities are indicative, though not definitively, of the milling process chemistry. In this case, $NaCl/H_2SO_4$ was used as an eluent for ion exchange and NaCl was also used in a solvent-extraction strip step. Similar to REEs, these trace elements and compounds are not an unambiguous signature but rather could be used as indicators for discerning aspects of the processing history of UOCs.

Degradation of UOCs. For UOCs, many of the chemical signatures and indicators that have been developed for nuclear forensics purposes are used to ascertain the origin of the uranium and sample processing history. One gap in the UOC signatures has been the development of chemical signatures associated with changes during handling, transport, and storage after production or when exposed to various environmental conditions. Several recent studies have focused on the development of these chemical signatures and indicators by studying uranium oxides subjected to controlled RH and temperature conditions.

Tamasi et al. studied several U_3O_8 samples, one pure U_3O_8 and two impure U_3O_8 samples, stored for 2−3.5 years in four different conditions: cool and dry (5 °C, 25% RH), cool and humid (5 °C, 97% RH), warm and dry (37 °C, 15% RH), and warm and humid (37 °C, 89% RH).[56] Using powder X-ray diffraction (p-XRD) and X-ray absorption fine structure (EXAFS) measurements, they analyzed the aged samples to identify changes in chemical speciation. For high-purity U_3O_8, no changes were observed during storage in dry conditions. However, for storage in humid conditions, two alteration phases were observed in the p-XRD patterns, the uranyl oxide hydroxyhydrates metaschoepite $[(UO_2)_4O(OH)_6](H_2O)_5$ and schoepite $[(UO_2)_4O(OH)_6](H_2O)_6$. It is important to note that metaschoepite and schoepite are often referred to by their empirical formulas, $UO_3{\cdot}2H_2O$ and $UO_3{\cdot}2.25H_2O$, respectively. The EXAFS data were consistent with the p-XRD data, indicating that little to no changes occurred in the samples aged under dry conditions, while there were significant changes in the samples aged in humid conditions consistent with the formation of schoepite ($UO_3{\cdot}xH_2O$) compounds, which included increased lattice disorder and changes in the U−O bond region. For the sample containing $UO_2F_2{\cdot}xH_2O$ as an impurity, schoepite compounds were formed after 2 years of storage in both dry and humid conditions. The other sample, which contained schoepite impurities at the onset, still contained schoepite compounds after 2 years of aging in both dry and humid conditions. Overall, this work demonstrated that U_3O_8 can convert to metaschoepite and schoepite during storage under humid environmental conditions. As a result, schoepite compounds could be used as a chemical indicator for ascertaining aspects of the postproduction history for U_3O_8.

Two recent studies have examined the effect of aging UO_2 under various humidity and temperature conditions. Donald et al. used X-ray photoemission spectroscopy (XPS) to identify changes in chemical speciation for high-purity UO_2 powder aged for approximately 1 year at 25 °C under various RH conditions (34%, 56%, and 98% RH; Figure 6).[51] The starting material contained primarily uranium(IV), as expected for UO_2, and a small portion of uranium(V). Over the course of the study, all samples underwent oxidation, as evidenced by a decrease in the relative amounts of uranium(IV) and uranium(V) and an increase in uranium(VI). After 378 days, the mean uranium valence for all samples was between U_3O_8 and UO_3. Interestingly, the authors concluded that the duration of storage, rather than the RH, had a greater effect on the extent of oxidation observed in the samples. The second study, conducted by Tracy et al., used grazing-incidence X-ray

https://doi.org/10.1021/acs.inorgchem.0c03390
Inorg. Chem. XXXX, XXX, XXX−XXX

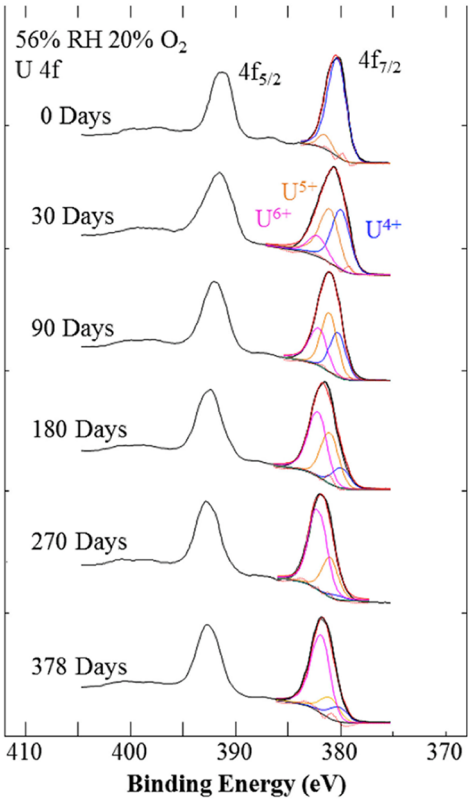

Figure 6. XPS U $4f_{7/2, 5/2}$ core-level spectra for aged UO_2 powders. Curve fits for the uranium(IV), uranium(V), and uranium(VI) valence states reveal that the sample underwent oxidation, as indicated by the increasing relative amount of uranium(VI) in the sample. Reprinted with permission from ref 51. Copyright 2017 Elsevier.

diffraction to study surface oxidation of the UO_2 samples aged under various RHs (34%, 56%, and 95% RH) and temperatures (room temperature, 50 °C, and 100 °C).[57] While surface oxidation was observed for the UO_2 samples, the authors determined that the RH did not significantly affect the extent of surface oxidation. However, they did observe a significant dependence on the temperature because the samples stored at 50 and 100 °C exhibited much thicker oxidized surface layers. Overall, both studies demonstrate that UO_2 will oxidize over time under environmental conditions; thus, higher valence uranium compounds could serve as indicators for aged UO_2 samples. However, the final chemical form of the oxidized UO_2 was not reported; thus, it is not known whether oxidation is the only chemical reaction taking place or whether hydration may also be involved, resulting in the formation of a uranium oxide hydrate compound, as observed in the studies considering U_3O_8.

One other UOC chemical form, UO_3, was recently studied by Wilkerson et al. to understand the effect of aging UO_3 under controlled humidity and temperature conditions for several years.[58] They used p-XRD and EXAFS to determine changes in chemical speciation in α-UO_3 samples stored in cool and dry (5 °C, 25% RH), cool and humid (5 °C, 97% RH), warm and dry (37 °C, 15% RH), or warm and humid (37 °C, 89% RH) conditions. After 14 months of storage, schoepite ($UO_3 \cdot xH_2O$) compounds were present in each α-UO_3 sample, except for the sample stored in cool and dry conditions. After 14 months of storage, they also observed an intermediate phase present in samples stored in both the cool and dry and the warm and dry conditions. Eventually, after 2.5 years of storage, all α-UO_3 samples contained schoepite compounds, demonstrating that, with sufficient storage time, α-UO_3 will eventually hydrate and transform into metaschoepite or schoepite. One aspect that differs from the other UOC chemical forms studied, UO_2 and U_3O_8, is that α-UO_3 is already in the uranium(VI) oxidation state, thus oxidation is not required for the formation of schoepite compounds. Similar to the study of U_3O_8, this study also indicates that schoepite compounds could serve as an indicator to provide insight into the postproduction history for UO_3 materials.

Aging studies for one final UOC chemical form, uranyl peroxide, are limited. As part of their U_3O_8 aging study, one sample Tamasi et al. investigated contained only studtite $[UO_2(O_2)\cdot 4H_2O]$ and metastudtite $[UO_2(O_2)\cdot 2H_2O]$ at the onset of the study.[56] Exposure to the various temperature and humidity conditions for up to 3.5 years only resulted in hydration of $UO_2(O_2)\cdot 2H_2O$ to $UO_2(O_2)\cdot 4H_2O$, and no other changes in chemical speciation were observed. Combining their results with the fact studtite and metastudtite have been observed in uranium deposits, it appears unlikely that studtite or metastudtite will be altered under humid conditions to form metaschoepite or schoepite.[78,79] However, recent investigations of storage drum pressurization incidents found that some uranyl peroxide UOCs contained a more reactive, amorphous uranium species. Odoh et al. found that certain uranyl peroxide UOCs were primarily *am*-U_2O_7, which results from drying $UO_2(O_2)\cdot 4H_2O$ or $UO_2(O_2)\cdot 2H_2O$ in air at approximately 300 °C.[55] Reacting this uranyl peroxide UOC with liquid water released O_2 and formed metaschoepite ($UO_3\cdot 2H_2O$). Given that aging U_3O_8 and UO_3 in humid conditions also leads to the formation of metaschoepite and schoepite, it is expected that a similar result will occur with uranyl peroxide UOCs containing a significant fraction of *am*-U_2O_7. The effect of varying the temperature and RH would likely be similar to the trends observed for U_3O_8 and UO_3, that is, exposure to more humid conditions will likely result in a more rapid transformation to metaschoepite. However, these hypotheses should be confirmed with a formal study of uranyl peroxide UOCs containing *am*-U_2O_7.

Advancing Analysis of UOCs. Several recent studies have investigated methods to improve the analysis of UOCs. Among other benefits, advancing analytical techniques for UOCs could lower limits of detection, expedite analysis timelines, or improve characterization of a sample, significant goals for nuclear forensics. Two recent studies investigated Raman spectroscopy for identifying UOCs. Pointurier et al. used micro-Raman spectroscopy (MRS) with two different excitation wavelengths (514 and 785 nm) to analyze micrometer-sized particles of uranium compounds and compared their observations with published spectra.[73] They acquired spectra for studtite $[UO_2(O_2)\cdot 4H_2O]$, U_3O_8, UO_2, and other uranium particles and found that they were consistent with the published spectra for bulk samples (Figure 7). Thus, they demonstrated the capability of identifying chemical speciation of uranium particles that were a few microns up to a few tens of microns in size. This is significant because certain samples collected for nonproliferation purposes by the International Atomic Energy Agency (IAEA), called swipe samples, may only contain micron-sized uranium particulate matter; MRS could be used to determine chemical speciation of uranium contained in these samples.[80] More recently, Ho et al. coupled Raman spectroscopy to multivariate analysis to visualize and

https://doi.org/10.1021/acs.inorgchem.0c03390
Inorg. Chem. XXXX, XXX, XXX−XXX

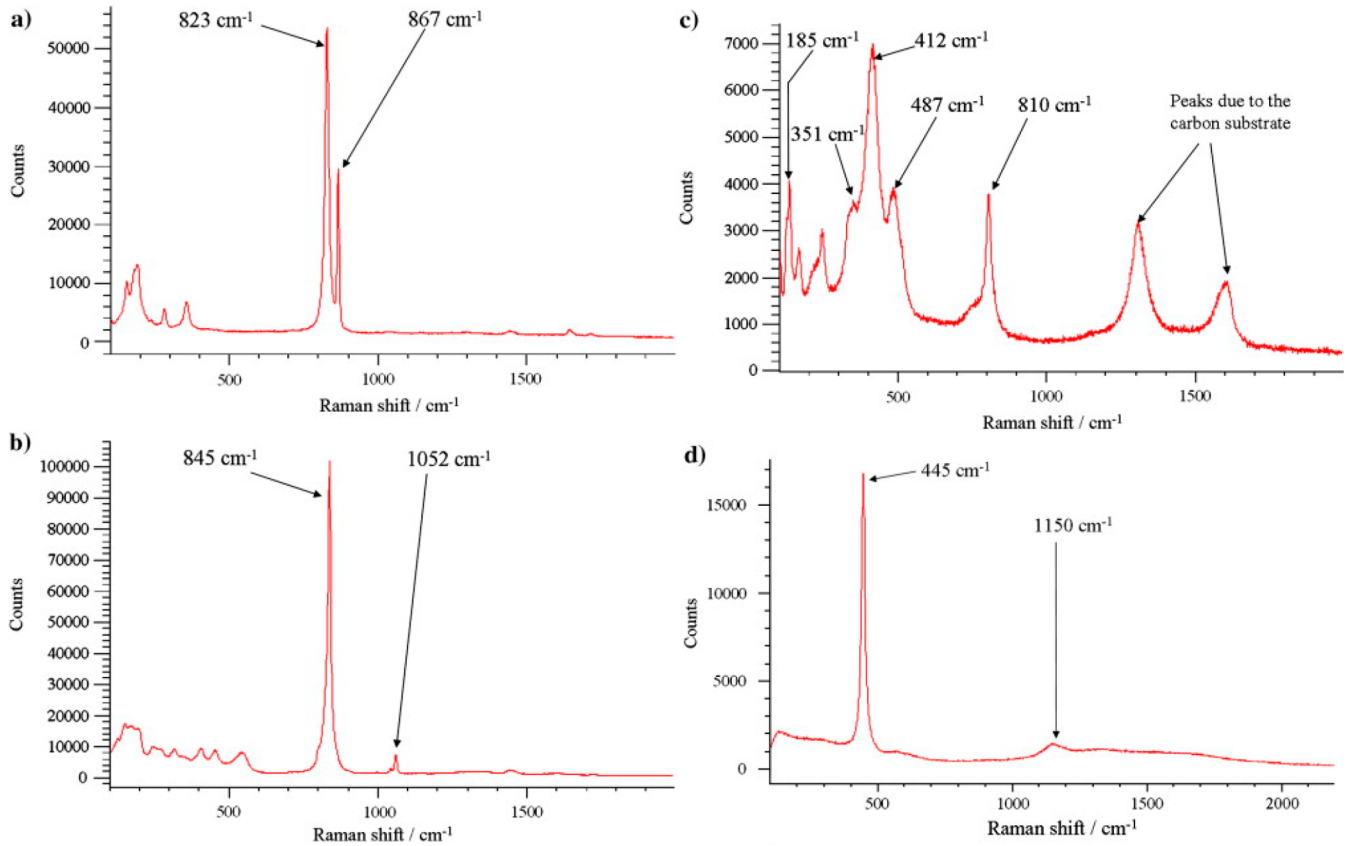

Figure 7. MRS spectra for micron-sized particles of various UOCs: $UO_2(O_2)\cdot 4H_2O$ (a), UO_3 (b), U_3O_8 (c), and UO_2 (d). Reprinted in part with permission from ref 73. Copyright 2010 Elsevier.

classify samples of UOCs.[72] They analyzed 89 industrially produced UOC samples along with 6 laboratory-prepared samples and processed this data set using three different multivariate analysis techniques: principal component analysis (PCA), partial least-squares discriminant analysis (PLS-DA), and Fisher discriminant analysis (FDA). Using PCA with three principal components, they found that certain compounds, including U_3O_8, uranyl peroxide, and AUC, could be grouped together in visual score plots. However, overlap was observed between clusters of the ADU and UH samples, limiting the ability to discriminate between these two UOCs. Using PLS-DA, they were able to better classify samples of AUC, U_3O_8, UO_3, and uranyl peroxide, an improvement over the results from PCA alone. Their results using FDA were similar, successfully grouping and discriminating some UOCs (ADU, U_3O_8, UO_3, UO_2, and uranyl peroxides), but not all were well separated. It is important to note that FDA is a supervised method that requires knowledge of a sample, thus limiting its usefulness for nuclear forensics analysis of unknown samples. They concluded that a combination of PCA and PLS-DA showed the greatest potential for rapidly and accurately classifying UOCs. Overall, these studies indicate that both MRS and multivariate analysis could be leveraged to enhance the analysis of UOCs for nuclear forensics purposes.

Another recent effort to discriminate between UOC chemical forms was conducted by Campbell et al. using LIBS.[70] LIBS is a rapid atomic emission technique and requires minimal sample preparation, offering an advantage over other, more time-intensive analytical methods. They prepared and analyzed three different UOC chemical forms: UO_2, U_3O_8, and UO_3. The samples were ablated using the same conditions to maintain a consistent amount of mass ablated between samples. Additionally, the samples were analyzed in an argon atmosphere to eliminate interference from atmospheric oxygen. The authors investigated several uranium emission lines as well as various laser power levels to determine whether they could successfully differentiate between the three uranium oxides based on the ratio of uranium and oxygen signal intensities. They observed different U/O signal intensity ratios between the three uranium oxides, consistent with the different uranium and oxygen contents for each compound. Among the various conditions studied, they determined that the 591.539 and 682.692 nm uranium emission lines and a 26 mJ laser power level provided the best discrimination between the three uranium oxides. Overall, this effort demonstrated the potential utility of LIBS to rapidly identify certain uranium compounds from a sample of material.

One final recent study investigated the chemical speciation in an ultrathin uranium oxide film using two nondestructive techniques. He et al. used neutron reflectometry (NR) and surface-enhanced Raman spectroscopy (SERS) to analyze a thin uranium oxide film, approximately 105 nm thick, deposited on a quartz substrate.[71] The NR results indicated that the film was composed of three sublayers: ~38 Å of α-U_3O_8, ~900 Å of α-UO_3, and ~115 Å of γ-UO_3. The SERS spectra were collected from optically pristine and optically damaged, as determined by SEM, locations on the thin film. The spectra collected from the pristine location was deconvolved and indicated that two phases were present in the film, γ-UO_3 and α-U_3O_8. The thick α-UO_3 layer was not

https://doi.org/10.1021/acs.inorgchem.0c03390
Inorg. Chem. XXXX, XXX, XXX−XXX

detected; this is likely because of the short-range effect of SERS. The spectra from the optically damaged sites showed additional bands and increased intensity of previously observed bands, associated with α-U_3O_8, confirming the existence of α-U_3O_8 in the sublayers of the uranium oxide film. Combining the results of both techniques, it was determined that the uranium oxide film was composed of an α-U_3O_8 layer on the quartz substrate followed by a thick α-UO_3 layer and a final, atmosphere-exposed layer of γ-UO_3. Overall, this study demonstrated a capability to determine depth-resolved, chemical speciation for an ultrathin film of uranium oxide using nondestructive techniques. Such a capability could provide physical and chemical data contained in ultrathin films, indicators that many current methods cannot access because they produce sample average properties.

Opportunities for Additional Research. As an easily transportable, and thus more easily trafficked form of uranium, UOCs warrant the significant amount of recent research. Yet, opportunities for additional research remain. To date, nearly all morphological studies of UOCs have focused on laboratory-prepared materials. Future studies investigating process samples from uranium mills and ISL mining would be beneficial for understanding morphological changes within an industrial setting, particularly how the morphology may be affected by varying process chemistry, and would help to build a database of reference materials from industrial facilities. Similarly, regarding trace elements in UOCs, the most significant future work is likely building a comprehensive database of reference materials by characterizing large numbers of process samples from uranium mills and ISL mining. Building a comprehensive database of the chemical and physical properties for UOCs produced globally should significantly improve nuclear forensics efforts to determine the origin and process history for uranium samples and also lay the groundwork to rigorously evaluate the utility of these potentially valuable methods by examining samples in the blind. As Ly et al. demonstrated with morphological analyses, the use of machine learning and data analytics will be key to effectively leveraging a comprehensive database of uranium material properties.[23,24] Regarding the degradation of UOCs, future studies should investigate the environmental degradation of uranyl peroxide and other UOCs, and similar to the morphological work, future studies should also study the degradation of process samples from uranium mills and ISL mining. Additionally, applying the morphology quantification tools to the environmentally driven morphological changes to UOCs may provide additional insight into the changes transpiring and improve the utility of morphological changes as an indicator for aspects of the postproduction history of UOCs. One more aspect of UOC degradation that would be very beneficial is determining the kinetics of the environmentally driven changes in chemical speciation; kinetic data would provide more quantifiable insights into the postproduction history of UOCs. With respect to advancing the analysis of UOCs, an opportunity for additional research is investigating the utility of techniques such as MRS and LIBS to identify the speciation of uranium material contained within a complex matrix collected for nonproliferation purposes.

URANIUM FLUORIDES UF_4 AND UF_6

From a nuclear forensics perspective, UF_4 and UF_6 are important because they are anthropogenic uranium compounds rarely encountered outside nuclear fuel production or nuclear weapons activities. Additionally, the primary use for UF_6 is the enrichment process. Enrichment is a technically challenging process within the front-end of the nuclear fuel cycle, and thus possessing an enrichment capability or attempting to establish an enrichment capability represents a significant milestone in producing nuclear reactor fuel or uranium suitable for weapons purposes. One tool used by the nonproliferation community, specifically the IAEA, is environmental sampling, which involves collecting swipe samples from declared or suspected nuclear facilities.[80] Forensic analysis of these samples is used to assess compliance, or noncompliance, with nuclear nonproliferation agreements. Finding UF_4 or the degradation products of UF_6 or UF_4 in a sample collected for nonproliferation purposes is a signature of anthropogenic uranium material and a strong indicator of an intent or capability to perform enrichment. In addition to nonproliferation-focused environmental samples, continued UF_4 and UF_6 research could identify chemical and physical characteristics useful for evaluating interdicted UF_4 or UF_6.

Trace Elements in UF_4 and UF_6. While significant research has focused on trace element forensics signatures in UOCs, as was already discussed, similar studies are noticeably scarce for UF_4 and UF_6 in the publicly available literature. Trace quantities of various elements are known to persist through the conversion of UOCs to UF_6, as indicated by the ASTM International C787 Standard Specification for Uranium Hexafluoride for Enrichment.[81] Some possible elemental impurities in UF_6 according to the ASTM C787 are listed in Table 1. The elemental impurities are grouped into two categories: those forming nonvolatile fluorides (vapor pressure of less than 101.3 kPa at 300 °C) and those forming volatile fluorides. A few notable elements within the list, based on nuclear-forensics-related studies for UOCs, are lead, molybdenum, and strontium. Noticeably absent from the list of potential elemental impurities in ASTM C787 are the REEs, which may also provide insights into the uranium's origin, as demonstrated with UOCs.[35,38,40,41] Analytical procedures for determining the lead, strontium, and REE impurities in UF_6 have been developed, but investigations to determine whether these methods are useful for nuclear forensics purposes, specifically aiding in determination of the origin of uranium, are not available in the literature.[82,83] While there is no analogous ASTM International standard specification for UF_4, the impurities expected for UF_6 represent a minimum subset of elemental impurities in UF_4 because it is an intermediate in the production of UF_6. It is unclear whether the REEs are present in UF_4 in addition to lead, molybdenum, and strontium. Additionally, investigations to determine whether lead,

Table 1. Potential Elemental Impurities in UF_6[a,81]

aluminum	*calcium*	**molybdenum**	*strontium*
antimony	*chlorine*	*nickel*	**tantalum**
arsenic	***chromium***	**niobium**	*thorium*
barium	*copper*	**phosphorus**	*tin*
beryllium	*iron*	*potassium*	**titanium**
bismuth	*lead*	**ruthenium**	**tungsten**
boron	*lithium*	**silicon**	**vanadium**
bromine	*magnesium*	*silver*	*zinc*
cadmium	*manganese*	*sodium*	*zirconium*

[a]Elements forming nonvolatile fluorides are italicized, and elements forming volatile fluorides are in bold.

https://doi.org/10.1021/acs.inorgchem.0c03390
Inorg. Chem. XXXX, XXX, XXX−XXX

molybdenum, strontium, or other elemental impurities in UF_4 are useful for nuclear forensics purposes, specifically aiding in determination of the origin of uranium, are not available in the literature.

In addition to scarce literature pertaining to trace elements in UF_4 and UF_6, an aspect of industrial-scale uranium conversion that would complicate the forensics of UF_4 and UF_6 is that UOCs from multiple geographic origins may be blended for processing at a conversion facility. Additionally, most facilities purify the uranium through solvent extraction at the beginning of the conversion process or via distillation of the final UF_6 product. These purification steps would likely alter or eliminate certain trace elemental impurities. Blending UOCs and employing a purification method, whether solvent extraction or distillation, could obscure geographically specific elemental and isotopic signatures. These complications illuminate a need to study UF_4 and UF_6 samples from the world's conversion facilities in order to understand the effect of blending UOCs and purification steps and, perhaps more importantly, identify the unique chemical characteristics of UF_4 and UF_6 produced at a given facility. In the event that trafficked UF_4 or UF_6 is interdicted, such knowledge could aid in identifying where it was produced or possibly indicate the existence of an undeclared conversion facility.

One recent study, by Reilly et al., considered trace element migration during uranium deconversion, specifically UF_4 reduction to uranium metal.[84] They prepared thorium-doped samples of UF_4, which were subjected to bomb reduction, yielding uranium metal. From a nuclear forensics perspective, thorium ingrowth from uranium decay, specifically ^{231}Th ingrowth from ^{234}U, can serve as a chronometer for the time that has elapsed since uranium was last quantitively separated from thorium.[85] Reilly et al. found that thorium did separate from the bulk uranium metal during bomb reduction; the fractionation ranged from 93 to 99%. For samples doped with less than 100 ppm of thorium, the fractionation was nearly quantitative, or nearly 100%. This study indicates that the thorium chronometer will be altered or reset during uranium deconversion using bomb reduction. This study also highlights the need to conduct additional research of trace elements in UF_4 to determine if other possible forensics signatures, such as origin data, may persist or be altered or destroyed during uranium deconversion.

Degradation of Uranium Fluorides in the Environment. There are very few published studies considering the degradation of UF_4 in the environment. One likely reason for the limited number of studies is that UF_4 is generally considered to be a stable compound.[86] Several studies have examined high-temperature hydrolysis, or pyrohydrolysis of UF_4, which converts UF_4 to uranium oxides of varying stoichiometries depending on the reaction conditions.[87−93] However, the reaction conditions for pyrohydrolysis, which proceeds at temperatures greater than 300 °C for UF_4, are not found in the environment. To date, Wellons et al. and Pointurier et al. have conducted the most extensive studies of UF_4 degradation under environmental conditions.[60,69] Using Raman spectroscopy, Wellons et al. identified the chemical transformation within UF_4 samples stored under varying RH conditions. They observed differing decomposition pathways, depending on the reaction conditions. At moderate RH (~50%), UF_4 was first converted to UO_2F_2, followed by a schoepite compound ($UO_3{\cdot}xH_2O$), and finally uranium oxide (U_xO_y). At higher RH (85%), UO_2F_2 was not observed, possibly because of deliquescence, but a schoepite compound and uranium oxide were. The first experiment was limited to approximately 2 weeks, but a 7-week experiment at both 57% and 77% RH resulted in the formation of a uranyl peroxide, metastudtite [$UO_2(O_2){\cdot}2H_2O$]. These two degradation pathways involve significant reactions including fluoride substitution, oxo bond formation, and uranium oxidation. Last, a simple experiment of mixing UF_4 in pure H_2O formed uranium tetrafluoride hydrate ($UF_4{\cdot}2.5H_2O$). On the basis of their observations, Wellons et al. proposed three, ambient-temperature hydrolysis schemes for the degradation of UF_4: eqs 1−3. Pointurier et al. investigated the degradation of micron-sized UF_4 particles (~5 μm diameter) stored in various conditions (humid or dry air, humid or dry argon, with or without UV exposure, and various temperatures) using MRS. While the duration of the study was limited to 3 months, they demonstrated that UF_4 microparticles degraded under certain conditions to form a schoepite or uranyl peroxide compound, similar to the observation by Wellons et al. In particular, storing UF_4 microparticles in a humid climate (>74% RH) led to the formation of a schoepite compound; adding UV light to the humid environment resulted in the formation of a uranyl peroxide. Increasing the temperature from 20 to 80 °C resulted in more rapid degradation. On the other hand, UF_4 microparticles stored under dry conditions, regardless of the temperature or UV exposure, exhibited no changes during the duration of the study. For the UF_4 microparticles that underwent degradation, UO_2F_2 was not observed, possibly because of deliquescence under the high-humidity conditions used for the study. Overall, their observations largely agree with the results from Wellons et al.

$$UF_4(\text{anhy}) \xrightarrow[-(HF)]{H_2O(g)} UO_2F_2{\cdot}2H_2O \xrightarrow[-(HF)]{H_2O(g)} UO_3{\cdot}xH_2O \xrightarrow{H_2O(g)} U_xO_y \quad (1)$$

$$UF_4(\text{anhy}) \xrightarrow[-(HF)]{H_2O(g)} UO_2F_2{\cdot}2H_2O \xrightarrow[-(HF)]{H_2O(g)} UO_4{\cdot}2H_2O \quad \text{longer duration} \quad (2)$$

$$UF_4 \xrightarrow{H_2O(l)} UF_4{\cdot}2.5H_2O \quad (3)$$

The observation that UF_4 degrades to UO_2F_2 is consistent with a recent UF_4 single-crystal study conducted by Tobin et al.[59] They observed significant degradation of the UF_4 crystal surface and identified the degradation product to likely be UO_2F_2 based on F K-edge (1s) X-ray absorption spectroscopy. The formation of a uranium oxide during the shorter-duration experiments by Wellons et al. is interesting considering the various studies demonstrating uranium oxides transforming into metaschoepite and schoepite discussed above; this observation warrants additional investigation.

While there are very few studies considering the environmental degradation of UF_4, the degradation of UF_6 in the environment is better understood. UF_6 does not react with O_2, N_2, or CO_2; however, it readily reacts with water (H_2O), both liquid water and water vapor in the air, making it unstable in the environment.[94] The reactivity of UF_6 toward water has been known since UF_6 was first synthesized in 1909, and the reaction yields both hydrogen fluoride (HF) gas and solid UO_2F_2, as shown in the overall reaction, eq 4.[94−96] Similar to the degradation of UF_4, the degradation of UF_6 involves

https://doi.org/10.1021/acs.inorgchem.0c03390
Inorg. Chem. XXXX, XXX, XXX−XXX

significant reactions including fluoride substitution and oxo bond formation. Atmospheric hydrolysis of UF_6 is more complicated than the reaction shown in eq 4. It has been suggested the hydrolysis reaction proceeds in two steps, eqs 5 and 6, forming an intermediate uranium oxytetrafluoride (UOF_4); however, the role of UOF_4 in this process remains debated.[97,98] Recently, Wagner et al. reportedly identified UOF_4 in particulate matter generated from reaction conditions with insufficient water for complete hydrolysis of UF_6.[99] However, compared to the reference Fourier transform infrared (FTIR) spectrum for UOF_4, their FTIR spectra do not strongly support this observation.[97]

$$UF_6 + 2H_2O \rightarrow UO_2F_2 + 4HF \quad (4)$$

$$UF_6 + H_2O \rightarrow UOF_4 + 2HF \quad (5)$$

$$UOF_4 + H_2O \rightarrow UO_2F_2 + 2HF \quad (6)$$

Computational studies by Hu et al. using relativistic density functional theory (DFT) indicate that the first hydrolysis reaction, eq 5, is composed of two steps, with UF_5OH as an intermediate (eqs 7 and 8).[100−102]

$$UF_6 + H_2O \rightarrow UF_5OH + HF \quad (7)$$

$$UF_5OH \rightarrow UOF_4 + HF \quad (8)$$

Recently, Richards et al. investigated the kinetics of UF_6 hydrolysis and determined that the rate appears to be half-order with respect to UF_6 and second order with respect to water, with a rate constant of 1.19 ± 0.22 $Torr^{-3/2}$ s^{-1} (eq 9).[98] Prior to this, one study reported a rate constant for UF_6 hydrolysis of $4 \pm 4 \times 10^{-18}$ cm^3 s^{-1}; however, limited experimental details were reported, and the rate constant was determined indirectly by measuring the ingrowth of HF, raising concerns regarding its validity.[103]

$$\text{rate} = k[UF_6]^{0.5}[H_2O]^2 \quad (9)$$

In addition to studies elucidating the atmospheric hydrolysis reaction scheme and kinetics, recent studies have investigated the effects of varying reaction conditions for UF_6 hydrolysis, with particular focus on the resulting UO_2F_2 particulate matter. When excess water is present, the UO_2F_2 product from UF_6 hydrolysis is a complex of $UO_2F_2{\cdot}xH_2O$ and HF, $UO_2F_2(H_2O)_x(HF)_y$.[63,104,105] HF is lost over time as the material equilibrates with the atmosphere, leaving the final product $UO_2F_2{\cdot}xH_2O$.[104,105] Two early studies considering the particle size and morphology of the UO_2F_2 particulate, conducted by Pickrell and by Lux, yielded somewhat contrasting findings.[106,107] Pickrell concluded that the RH and aerosol incubation period, or growth time, affected the particle size and morphology of the resulting UO_2F_2 particulate, whereas Lux found the particle size distribution of the UO_2F_2 particulate matter to be largely unaffected by varying humidity. To help resolve this disagreement, recent work by Kips et al. used SEM to study the effect of humidity on the UO_2F_2 particle morphology.[63] They performed UF_6 hydrolysis reactions in an aerosol deposition chamber at ∼68%, ∼43%, and ∼15% RH. The particles formed at ∼68% RH were primarily discrete spheroids ranging in size from 0.5 to 2.25 μm, although 95% of the particles were smaller than 1.5 μm and ∼70% were smaller than 1 μm. The particles exhibited no agglomeration and were well separated. For hydrolysis of UF_6 in high-humidity conditions, the resulting UO_2F_2 particles may absorb water during formation and deposition, causing the highly spherical particle shape. The particles formed at ∼43% RH were not spherical but irregularly shaped and did not exhibit agglomeration. Further reducing the humidity to ∼15% primarily produced chainlike agglomerated particles. Particle size distributions were not provided for the ∼43% and ∼15% RH reaction conditions. Overall, the observations of Kips et al. compare more favorably with Pickrell's observations than those of Lux. Recently, Cheng et al. studied the formation and growth of primary UO_2F_2 particles produced by gas-phase hydrolysis of UF_6.[108] For the conditions investigated, they found UO_2F_2 primary particle formation and growth was strongly dependent on the H_2O molecules available. Higher-humidity conditions resulted in larger primary particle sizes with a peak aerosol mobility diameter of approximately 8 nm, whereas water-deprived reaction conditions produced smaller primary particles with a peak aerosol mobility diameter of approximately 3.6 nm. Sampling at three points along the reaction chamber indicated that growth of the primary particles with respect to time as they traversed the reaction chamber and higher-humidity conditions resulted in an increased growth rate. These results may seem to contrast with the observations of Pickrell and Kips et al.; however, Cheng et al. measured primary particles that serve as the seed for additional particle growth, whereas Pickrell and Kips et al. measured the final particle sizes. Overall additional investigations of gas-phase UF_6 hydrolysis are warranted to better understand primary particle and agglomerated particle formation. There are several more studies focused on UO_2F_2 particulate matter resulting from UF_6 hydrolysis, and those studies are addressed in the UO_2F_2 section of this paper.

Opportunities for Additional Research. As the only uranium compound used for industrial-scale enrichment, UF_6 fulfills a pivotal role in the nuclear fuel cycle. Unfortunately, the inherent instability of UF_6 limits the opportunities for additional nuclear-forensics-focused UF_6 research. One area that may warrant additional investigation is trace element signatures in UF_6. As outlined in the ASTM specification for UF_6, various elemental impurities found in UOCs may persist through the uranium conversion process into the UF_6 product. Research into these impurities may identify chemical signatures useful for determination of the provenance and history of UF_6 materials. As discussed, such research could be greatly bolstered by investigating UF_6 samples from the various uranium conversion facilities around the globe.

Unlike UF_6, there are more readily apparent opportunities for nuclear-forensics-focused UF_4 research. Because UF_4 is more stable in the environment than UF_6, morphological research, akin to the current efforts focused on the morphology of UOCs, may more easily identify the origin and history signatures for UF_4 materials. Because of the limited number of studies available, additional investigations into the degradation of UF_4 in the environment are warranted, in particular, longer-duration studies considering a wide range of environmental conditions. Similar to UF_6, an investigation of the trace element signatures in UF_4, bolstered by the characterization of samples from conversion facilities, may identify signatures useful for determining the source and history of UF_4 materials. Last, in addition to being an intermediate product during uranium conversion, UF_4 may be produced as an intermediate during UF_6 deconversion to uranium metal via reaction with a reducing agent such as hydrogen (eq 10). Investigations of UF_4 produced by both processes may identify signatures or indicators, such as morphological features or trace elements,

https://doi.org/10.1021/acs.inorgchem.0c03390
Inorg. Chem. XXXX, XXX, XXX−XXX

that could differentiate between UF_4 produced during uranium conversion and UF_4 produced during uranium deconversion.

$$UF_6 + H_2 \rightarrow UF_4 + 2HF \quad (10)$$

UO_2F_2

As an intermediate during certain fuel fabrication or UF_6 deconversion processes, UO_2F_2 appears at first to be an insignificant uranium compound within the front-end of the nuclear fuel cycle. However, from a nuclear forensics perspective, UO_2F_2 is important because it is a stable anthropogenic uranium compound rarely encountered outside nuclear fuel production or weapons activities. Moreover, because it is the immediate hydrolysis product of UF_6 and may also be formed by the environmentally driven degradation of UF_4, UO_2F_2 is a key chemical signature of nuclear-related activities handling UF_4 or gaseous UF_6.[60,109] For example, finding UO_2F_2 in a swipe sample collected for nonproliferation purposes is a strong indicator that UF_6 or UF_4 was previously present. Because it is important for nonproliferation nuclear forensics, recent research has focused on characterizing UO_2F_2 particulate matter, understanding how it degrades in the environment, and developing analytical techniques that could be used to identify it from environmental samples or through remote monitoring.

Analysis of UO_2F_2 Particulate. There have been a few recent vibrational spectroscopy studies of UO_2F_2 particulate created by hydrolysis of UF_6 (eq 4), primarily using MRS. Kips et al. studied UO_2F_2 created in an aerosol deposition chamber, ranging in size from 0.1 to 1 μm diameter, deposited on graphite planchets.[61,64] They observed the intense uranyl stretching peak at either 865 or 863 cm^{-1} and the weaker U−O bending peak around 180 cm^{-1}. For reference, the range of symmetric uranyl stretching frequencies is approximately 800−900 cm^{-1} for various uranyl compounds.[110] Pointurier and Marie studied larger-sized (several microns) UO_2F_2 particles using MRS.[73] The larger particle sizes enhanced the Raman signal, increasing the intensity of the strong uranyl stretching peak at 867 cm^{-1} and the weaker U−O bending peak at 180 cm^{-1} (Figure 8). Stefaniak et al. also studied UO_2F_2 created in the aerosol deposition chamber used by Kips et al. but deposited on various types of planchets.[111] They found that silver foil, stainless steel, and gold planchets enhanced the Raman signal relative to graphite planchets, with gold resulting in the greatest enhancement. Enhancing the Raman signal increased the peak intensity of both the intense uranyl stretching and weaker U−O bending peaks. They also observed that the intense uranyl stretching peak shifted to lower frequencies. For particles deposited on silver foil, the uranyl peak was observed as a double peak at 863 and 848 cm^{-1}, for gold at 842 cm^{-1}, and for stainless steel at 839 cm^{-1}. The shifts in the peak positions may be due to increased hydration of the UO_2F_2 particles or degradation because the samples were stored in ambient conditions and possibly interaction between the particles and planchet material. Overall, the vibrational spectroscopy studies of UO_2F_2 particulates demonstrate that the material is at least partially hydrated. Varying the planchet substrates may affect analysis of the UO_2F_2 particulate material and could potentially be leveraged to improve detection limits.

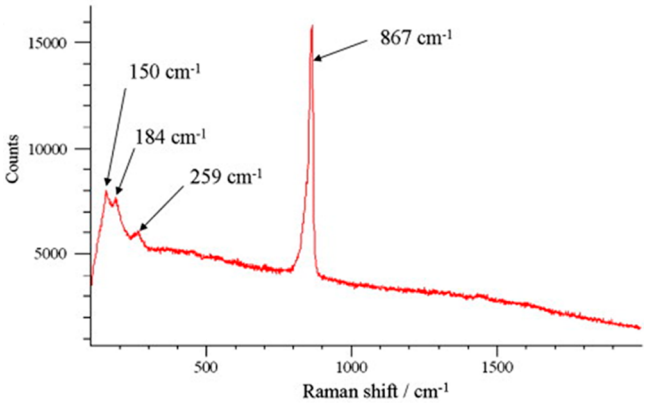

Figure 8. MRS spectra for micron-sized particles of UO_2F_2. Reprinted in part with permission from ref 73. Copyright 2010 Elsevier.

In addition to MRS, Kips et al. investigated UO_2F_2 particles using energy-dispersive X-ray (EDX) spectroscopy, secondary-ion mass spectrometry (SIMS), and cryogenic laser-induced fluorescence spectroscopy (CLIFS).[63,112] The EDX spectrum of freshly prepared particles clearly indicated the presence of both oxygen and fluorine based on their respective Kα lines. The SIMS data showed several peaks attributable to combinations of uranium and fluorine atoms or uranium, oxygen, and fluorine atoms (Table 2). As seen in Table 2, some isobaric interferences from peaks attributable to a combination of only uranium and oxygen, specifically the peaks at mass 254 and 270, may obfuscate the more important signals from fluorine-containing species. The CLIFS spectrum showed two sets of peaks; the first set (502, 523, 545, and 578 nm) was significantly more intense than the second set (515, 539, 564, and 590 nm). The set of intense peaks agrees favorably with the previously published fluorescence studies for UO_2F_2 solutions.[113,114] Kips et al. tentatively interpreted the less intense set of peaks as arising from one or more waters of hydration, but they also mentioned the possibility that the second set of peaks was from a schoepite-like compound. Considering the findings from Kirkegaard et al. discussed in the next section of this paper, it is likely that the second set of less intense peaks is from a schoepite-type compound.[66]

Table 2. SIMS Peaks Attributable to Fluorine-Containing Species[63,112]

mass	peak attribution
254	^{235}UF or ^{238}UO
257	^{238}UF
270	^{235}UOF or $^{238}UO_2$
273	^{238}UOF or $^{235}UF_2$
276	$^{238}UF_2$

Overall, these studies demonstrate the ability to probe micron-sized UO_2F_2 particles using a variety of analytical techniques. The demonstrated analytical methods are effective for determining the physical characteristics of the particulate matter and identifying elements present in the particle. However, while EDX and SIMS can provide elemental data for a particle, they do not necessarily verify that the particle is or contains UO_2F_2, but rather uranium, oxygen, and fluorine are present in the particle. For nuclear forensics purposes, proving the presence of UO_2F_2 is significant. In this regard, MRS and CLIFS stand out as potential means to identify UO_2F_2 in a particle using the strong uranyl stretching peak or

https://doi.org/10.1021/acs.inorgchem.0c03390
Inorg. Chem. XXXX, XXX, XXX−XXX

fluorescence peak pattern, respectively. Furthermore, combining EDX or SIMS elemental data with MRS and/or CLIFS could increase confidence in positively identifying UO_2F_2.

Degradation of UO_2F_2. UO_2F_2 is known to degrade, presenting a challenge to using it as a chemical signature for nuclear forensics purposes. For example, Kips et al. observed the absence of fluorine in the EDX spectrum and SIMS data from UO_2F_2 particles that were heat treated at 350 °C for 6 h.[63] This is consistent with previous observations that UO_2F_2 undergoes thermal decomposition and sublimation at elevated temperatures.[115−118] While this temperature is not found within the terrestrial environment, this degradation is problematic because heat treatment may be used to burn off potentially interfering organic compounds from samples collected for nuclear forensics purposes. Several studies have investigated the degradation of UO_2F_2 particulate in order to better understand the effect of varying conditions on the rate and mechanism of the process.

Expanding on the observed fluorine loss from heat-treated UO_2F_2 particles, Kips et al. conducted a more extensive aging study to assess the effect of humidity and UV exposure on fluorine loss.[64,65] Using a variety of analytical techniques including SEM−EDX, SIMS, and MRS, they examined UO_2F_2 particles synthesized at varying levels of humidity and stored for varying lengths of time (1 week to 28 months). In addition to variation of storage timelines, a few samples were exposed to several weeks of intense UV light. Using SIMS, they measured the $^{238}UF^+/^{238}U^+$ (257/238) ratio of samples shortly after sample preparation or after storage. The ratio generally decreased by approximately 1 order of magnitude for samples stored for 11−28 months, indicating that fluorine loss occurred during that storage period. For the aged particles, the SEM−EDX spectrum showed a small, but discernible peak for the F Kα line and the MRS spectrum also showed a discernible peak at 866 cm^{-1}, characteristic of UO_2F_2. For the samples exposed to 3−4 weeks of continuous UV light, the $^{238}UF^+/^{238}U^+$ ratio also decreased by approximately 1 order of magnitude, indicating that several weeks of UV-light exposure results in fluorine loss comparable to that of storage for 11 to 28 months. Like the aged particles, the SEM−EDX spectrum did show a small, but discernible peak for the F Kα line and the MRS spectrum also showed a discernible peak at 865 cm^{-1}. They extended the UV-exposure study to 3 months and found that the $^{238}UF^+/^{238}U^+$ ratio decreased to near the SIMS detection limit. Additionally, fluorine was not observed in the SEM−EDX spectrum; however, the MRS spectrum did show a peak at 865 cm^{-1}.

Next, Kips et al. investigated fluorine loss during storage under varying levels of humidity.[61,62] Using SIMS and MRS, they analyzed UO_2F_2 particles stored in an inert atmosphere, dry air (<15% RH), moderately humid air (30−43% RH), and high-humidity air (70−76% RH). Using SIMS, they measured the $^{19}F^+/^{238}U^+$ ratio for the particles, and while there was large variability of the measured ratio for each storage condition, their results demonstrate a general trend that increasing humidity tends to increase fluorine loss. Using MRS, they observed the strong uranyl stretching peak at 865 or 863 cm^{-1} for samples stored in an inert atmosphere.[61,62] The MRS spectrum for particles stored in dry air showed the uranyl stretching peak at around 863 cm^{-1} and an additional peak around 845 cm^{-1}, likely also from uranyl stretching. The spectrum for samples stored in moderately humid air also showed uranyl stretching peaks at around 863 cm^{-1} and 845 cm^{-1}. Last, the spectrum from samples stored in high-humidity air only showed the uranyl stretching peak at around 843 cm^{-1}. Additionally, the MRS spectra of the samples showed broadening of the uranyl stretching peak, except for the samples stored in an inert atmosphere. These results indicate that the degradation of UO_2F_2 due to humidity results in peak broadening and shifting of the uranyl stretching peak to lower frequencies. Kips et al. postulated that the peak broadening and shifting may be attributed to a change in the hydration state.

More recently, Kirkegaard et al. investigated the degradation of UO_2F_2 using MRS.[67] They stored UO_2F_2 particle samples at approximately 75% RH and collected the MRS spectrum multiple times during the storage period. The initial MRS spectrum showed the expected uranyl stretching peak near 868 cm^{-1}. Over the course of storage, two additional peaks appeared in the spectra, 845 and 820 cm^{-1}, growing in intensity, while the UO_2F_2 868 cm^{-1} peak decreased in intensity. After 190 days of storage, one set of samples was moved to storage in approximately 100% RH, and this resulted in growth of the peak at 820 cm^{-1}, a decrease of the peak at 845 cm^{-1}, and growth of a peak at 866 cm^{-1}. Deconvolution of the spectra suggests that three species were present over the course of the study. The first was the starting $UO_2F_2{\cdot}xH_2O$. On the basis of the frequency of the uranyl stretching peak and loss of fluorine, the authors suggest that the second species is a uranyl hydroxide hydrate, akin to schoepite, and the final species is a uranyl peroxide. The appearance of the peak at 845 cm^{-1} is consistent with the observations of Kips et al. but had not been postulated to arise from a non-UO_2F_2 species.

Next, Kirkegaard et al. extended their investigation of UO_2F_2 degradation, increasing the range of RH storage conditions and adding p-XRD analysis of aged bulk UO_2F_2 material.[66,68] For this study, several samples were stored under controlled temperature (25 or 35 °C) and varying RH (32−94.6% RH) for 220 days and the p-XRD sample was stored at 35 °C and high RH (>83%) for 247 days. The initial MRS spectra of all samples matched that of hydrated UO_2F_2. For the samples stored in greater than 33% RH, they observed changes to the MRS spectra consistent with their previous study. For the two samples stored in less than 33% RH, their MRS spectra remained unchanged, which indicates that UO_2F_2 particles are relatively stable when stored under these conditions. This result seems to contrast the earlier-discussed observations of Kips et al. for samples stored in dry conditions (<15% RH); however, Kips et al. reported that, following the initial fluorine loss during the first several weeks of storage in dry air, the fluorine loss for UO_2F_2 was minimal on a yearlong time scale, indicating that the decomposition had stabilized or occurred at a very slow rate.[62] The p-XRD pattern of the initial bulk material matched favorably with the expected hydrated UO_2F_2 pattern. The p-XRD pattern collected at 76 days matched favorably with a uranyl oxide hydroxyhydrate species, and the pattern collected at 247 days matched a combination of a uranyl oxide hydroxyhydrate species, studtite ($UO_2(O_2){\cdot}4H_2O$) and metastudtite ($UO_2(O_2){\cdot}2H_2O$) (Figure 9). These results are consistent with the MRS observations from their previous degradation study. On the basis of their observations, the degradation of $UO_2F_2{\cdot}xH_2O$ in the presence of sufficient H_2O follows the reaction scheme shown in eq 11.

https://doi.org/10.1021/acs.inorgchem.0c03390
Inorg. Chem. XXXX, XXX, XXX−XXX

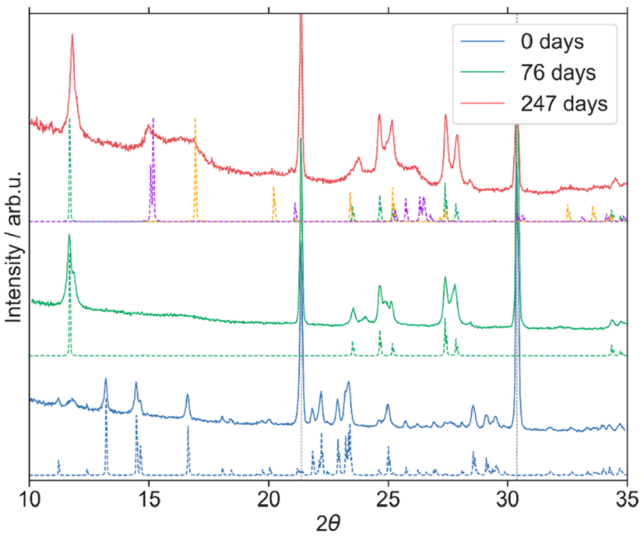

Figure 9. Time resolved p-XRD patterns for $[(UO_2F_2)(H_2O)]_7 \cdot (H_2O)_4$ stored at 35 °C and 85% RH. p-XRD reference patterns are shown for $[(UO_2F_2)(H_2O)]_7 \cdot (H_2O)_4$ (blue), a previously characterized uranyl hydroxide hydrate (green),[68] studtite $(UO_2(O_2) \cdot 4H_2O)$ (purple), and metastudtite $(UO_2(O_2) \cdot 2H_2O)$ (orange). The intense peaks at 2θ = 21.36° and 30.38° correspond to a LaB_6 standard. Reprinted in part with permission from ref 66. Copyright 2020 Elsevier.

$$[(UO_2F_2)H_2O]_7 \cdot 4H_2O \xrightarrow{H_2O(g)} UO_3 \cdot xH_2O \xrightarrow{H_2O(g)} UO_2(O_2) \cdot xH_2O \quad (11)$$

Last, Kirkegaard et al. used the MRS data from their extended investigation to provide insight into the kinetics and mechanism for UO_2F_2 degradation.[66] They observed a sigmoidal shape of the UO_2F_2 concentration curves for each particle, indicating a decelerating rate of conversion over time. This observation suggests a denucleation-driven degradation. They propose that the degradation mechanism involves absorbed water interacting with the fluorine ligands, causing the fluorine ligand to dissociate. The dissociated fluorine ligand is replaced with a hydroxy ligand, and the newly formed HF leaves the crystal lattice. On the basis of extrapolation of the data for 25 °C, they also observed slower than expected reaction rates for the samples stored at 35 °C. They suggest that this is likely due to the effect of temperature on the water sorption isotherm, where increasing temperatures reduce the amount of absorbed water. Decreasing the amount of absorbed water decreases interactions with the fluorine ligands, negatively impacting the reaction rate.

Overall, the various degradation studies demonstrate that UO_2F_2 will lose fluorine with time when exposed to various environmental conditions. High temperatures and intense UV-light exposure evidently accelerate the loss of fluorine, and, in general, the data suggest that exposure to high levels of humidity also accelerates the loss of fluorine. Because of some disagreement between studies, the effect of exposure to low levels of humidity is less clear. The gathered literature suggests that there is a humidity level below which UO_2F_2 only partially degrades or the degradation is practically negligible. Additional studies will be necessary to more definitively determine the degradation of UO_2F_2 exposed to low levels of humidity. Additionally, the reported formation of uranyl peroxide by Kirkegaard et al. warrants additional investigation because their samples were protected from light. The radioactivity of natural uranium deposits has been shown to produce sufficient H_2O_2 via radiolysis of water to cause the formation of uranyl peroxide.[79] However, their experimental setup used depleted uranium, which is less radioactive, raising questions as to whether it can produce sufficient H_2O_2 via radiolysis to cause the formation of uranyl peroxide. A depleted uranium projectile corroded in soil for 7 years was shown to contain uranyl peroxide, but given the shorter duration of the Kirkegaard et al. aging study, there is no readily apparent mechanism for peroxide formation in their system.[119] From the perspective of nonproliferation nuclear forensics, degradation of UO_2F_2 results in the loss of this important chemical signature and therefore places constraints on when and how environmental samples of interest should be acquired and handled. Primarily, environmental samples would need to be collected within an appropriate period after UO_2F_2 particulate is formed, they should be stored in dry and inert conditions to preserve any UO_2F_2 that may be present, and they should be processed and analyzed quickly to minimize degradation. Importantly, for analysis purposes, an environmental sample would need to be processed in a manner that prevents or minimizes degradation of UO_2F_2. On the other hand, the eventual degradation of UO_2F_2 in the environment means that any detected particle is likely from recent and/or nearby activities and not part of a background signature.

Advancing Techniques for UO_2F_2 Detection. Techniques for detecting and identifying UO_2F_2 through remote monitoring or within complex matrixes, such as soil or sand, would be invaluable for nuclear forensics purposes. For example, remote monitoring could help to overcome time constraints imposed by the degradation of UO_2F_2 particulate, and, similarly, identifying UO_2F_2 particulate within a complex matrix could significantly expedite analysis of environmental samples. Several analytical techniques have been investigated as possible means to achieve these aims.

An early investigation of remote monitoring by Bostick et al. was focused on worker safety rather than nuclear forensics.[104] They attempted to use Raman laser spectroscopy to monitor the uranyl stretching frequency at 868 cm^{-1} during an experimental UF_6 release but were unable to obtain a signal distinguishable from the background. They did successfully use IR laser spectroscopy tuned to the uranyl stretching absorption at 855 cm^{-1} to monitor the UF_6 release; however, the sensitivity was approximately 1 order of magnitude lower than the sensitivity of a nonspecific light scattering method used to detect the aerosol. The limit of detection for the IR technique was not investigated, and it used a relatively short path length (60 cm); these factors could limit its applicability to safety monitoring rather than remote detection for nuclear forensics.

More recently, Shattan et al. investigated the use of LIBS to detect UO_2F_2 within a mixture of UO_2F_2 and sand.[74] Using a commercially available hand-held LIBS system, the authors detected UO_2F_2 using four uranium emission lines and determined that the limit of detection for the studied system is 250 ppm. This study demonstrated the capability to detect uranium within a relevant environmental sampling matrix, sand. However, LIBS is an elemental analysis technique and thus, in this study, detects uranium in the matrix and not specifically UO_2F_2. While the detection of small quantities of uranium in a sand matrix is useful, the ability to identify the

https://doi.org/10.1021/acs.inorgchem.0c03390
Inorg. Chem. XXXX, XXX, XXX−XXX

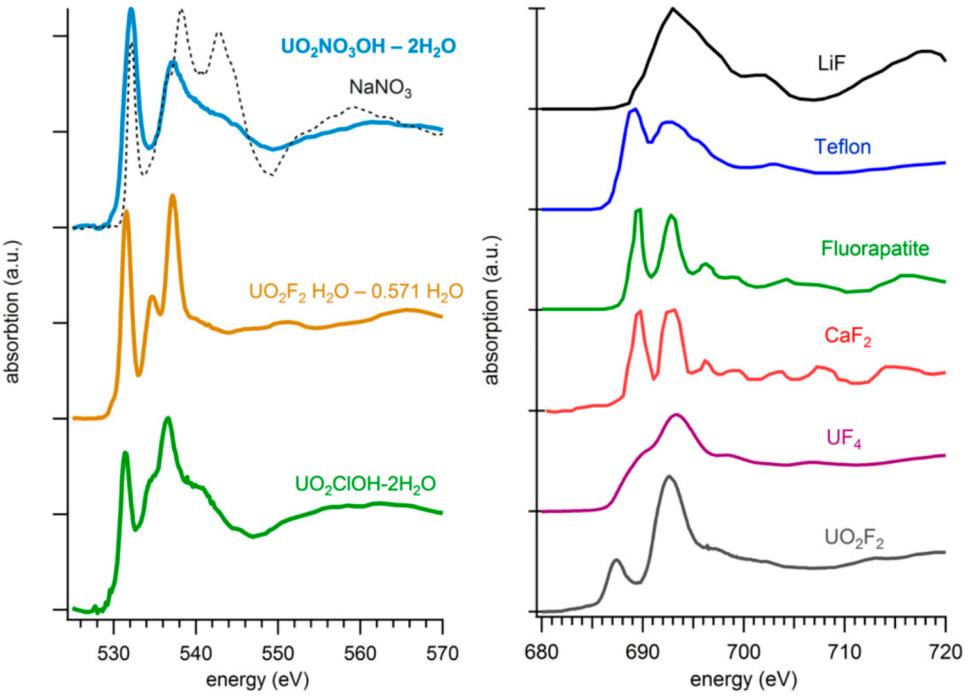

Figure 10. Comparison of the O K-edge (left) and F K-edge (right) absorption spectra demonstrating the ability to distinguish UO_2F_2 from pertinent nuclear fuel cycle compounds (uranyl nitrate, uranyl chloride, and UF_4) and fluorine-containing compounds that could be encountered in the environment (fluorite and fluorapatite) or laboratory (Teflon and lithium fluoride). Reprinted with permission from ref 76. Copyright 2017 Elsevier.

UO_2F_2 compound would be significantly more beneficial for nuclear forensics purposes. Adding the capability to simultaneously detect fluorine may improve the value of LIBS as a screening tool, but the conclusion of simultaneously detecting uranium and fluorine using LIBS would be limited to the presence of both elements within the ablation spot size, not necessarily that the sample contains UO_2F_2.

Ward et al. studied UO_2F_2 using soft X-ray near-edge absorption spectroscopy; specifically, they used O K-edge and F K-edge absorption spectroscopy to analyze UO_2F_2 (Figure 10).[76] They demonstrated that O K-edge absorption spectroscopy could distinguish UO_2F_2 from two other uranyl compounds relevant to the nuclear fuel cycle ($UO_2NO_3OH{\cdot}2H_2O$ and $UO_2ClOH{\cdot}2H_2O$). They also demonstrated that F K-edge absorption spectroscopy could distinguish UO_2F_2 from potentially interfering fluorine-containing compounds that could be encountered in the nuclear industry (UF_4), environment (fluorite and fluorapatite), or laboratory (Teflon and lithium fluoride). Their measurements were made on bulk samples, but the measured spectra may be used to interpret spectra from spatially resolved techniques such as scanning transmission X-ray microscopy.

Last, Skrodzki et al. considered coupling laser-induced fluorescence (LIF) spectroscopy to ultrafast laser filamentation to enable remote detection of UO_2F_2.[75] Filamentation has been shown to enable energetic femtosecond laser pulses to propagate up to 1 km. Their study investigated the excitation of UO_2F_2 (0.05 M UO_2F_2 in 0.05 M HF/0.05 M KF) using an ultrafast laser to determine its fluorescence signature under such excitation conditions. The resulting fluorescence spectrum showed five peaks with peak positions consistent with previous LIF studies of UO_2F_2, and they determined that the luminescence decay rates for the five peaks were in the range of $(4.3–5.6) \times 10^4$ s^{-1}. Next, they investigated the excitation of UO_2F_2 following optical filamentation of laser radiation. They determined that the luminescence decay rates for the five fluorescence peaks were similar to those observed for ultrafast excitation, $(4.4–5.5) \times 10^4$ s^{-1}. This study demonstrated the ability to reproduce the results from LIF spectroscopy using ultrafast laser filamentation excitation. This study suggests that remote detection of UO_2F_2 may be feasible using ultrafast laser filamentation-induced fluorescence spectroscopy; however, it was a benchtop study with minimal atmospheric interferants and a short path length, not representative of a remote detection scenario. Additionally, the limiting analyte concentration for this system was not investigated nor was the impact of analyzing aerosolized rather than dissolved UO_2F_2. Thus, it is unknown what concentration of UO_2F_2 would be required in order to be detected in a remote scenario.

Overall, these various studies have identified techniques that could potentially be used for detecting and identifying UO_2F_2 through remote monitoring or within complex matrixes; however, significant work remains. Setting aside the nonspecific (light-scattering) and elemental (LIBS) techniques, the other studies stop short of proving the capability in a real-world scenario, such as long-distance path lengths or complex environmental sample matrixes. More real-world conditions will likely frustrate these analytical methods, but the hindrances may be surmountable.

Opportunities for Additional Research. Recent UO_2F_2 research has been spurred by its importance for nuclear forensics as a chemical signature of activity handling gaseous UF_6. To date, most of the nuclear-forensics-related research has focused on understanding the environmentally driven degradation of UO_2F_2 as well as detecting and identifying UO_2F_2 remotely or within a complex matrix. Opportunities for additional research include continued efforts to advance analytical techniques such as MRS and LIBS in order to

https://doi.org/10.1021/acs.inorgchem.0c03390
Inorg. Chem. XXXX, XXX, XXX−XXX

detect UO_2F_2 through remote monitoring or within a nonproliferation sample medium such as a swipe sample. A complementary research opportunity, pertinent to nonproliferation efforts, is the development of a separation technique to isolate UO_2F_2 from environmental sampling media. Separating UO_2F_2, while maintaining the UO_2F_2 chemical speciation, could enable the detection of smaller quantities of UO_2F_2 particulate, effectively reducing the UO_2F_2 limit of detection for environmental samples and ultimately leading to improved nuclear forensics capabilities.

CONCLUSIONS

Uranium compounds associated with the front-end of the nuclear fuel cycle have witnessed a surge of research over the past decade, driven by the growing importance of nuclear forensics. Overall, this effort has furthered the chemistry of these uranium compounds and resulted in significant forensics-relevant results. In particular, the characterization of uranium compounds' morphologies, including their persistence and alteration through various reactions, has grown significantly. Additionally, the degradation of uranium compounds under environmentally relevant conditions is better understood. Last, various analytical methods including MRS, LIBS, and advanced X-ray and neutron spectroscopic techniques have been demonstrated as valuable capabilities for accessing forensically relevant chemical and physical characteristics of uranium samples.

While this recent research has yielded significant results, opportunities for further work remain. For UOCs, future work investigating morphological characteristics and environmental degradation should consider process samples from industrial uranium mills and ISL mining, building on the foundation of results from laboratory-prepared samples. For uranium fluorides, research opportunities include investigating trace element impurities, and for UF_4 specifically, future research should more thoroughly investigate its degradation under environmental conditions as well as morphological characteristics, akin to the morphological work accomplished for UOCs. With respect to UO_2F_2, future research opportunities include the development of analytical techniques capable of detecting UO_2F_2 remotely or within a complex matrix, as well as the development of a separations technique to drive down detection limits for UO_2F_2 in environmental samples. Overall, the importance of nuclear forensics for nuclear nonproliferation efforts will likely continue to drive uranium research efforts.

AUTHOR INFORMATION

Corresponding Author

Jenifer C. Shafer − *Department of Chemistry and Nuclear Science and Engineering Program, Colorado School of Mines, Golden, Colorado 80401, United States;* orcid.org/0000-0001-9702-1534; Email: jshafer@mines.edu

Authors

Kevin J. Pastoor − *Department of Chemistry, Colorado School of Mines, Golden, Colorado 80401, United States*

R. Scott Kemp − *Department of Nuclear Science and Engineering, Massachusetts Institute of Technology, Cambridge, Massachusetts 02139, United States*

Mark P. Jensen − *Department of Chemistry and Nuclear Science and Engineering Program, Colorado School of Mines, Golden, Colorado 80401, United States*

Complete contact information is available at: https://pubs.acs.org/10.1021/acs.inorgchem.0c03390

Notes

The authors declare no competing financial interest.

Disclaimer: This report was prepared as an account of work sponsored by an agency of the United States Government. Neither the United States Government nor any agency thereof, nor any of their employees, makes any warranty, express or implied, or assumes any legal liability or responsibility for the accuracy, completeness, or usefulness of any information, apparatus, product, or process disclosed, or represents that its use would not infringe privately owned rights. Reference herein to any specific commercial product, process, or service by trade name, trademark, manufacturer, or otherwise does not necessarily constitute or imply its endorsement, recommendation, or favoring by the United States Government or any agency thereof. The views and opinions of authors expressed herein do not necessarily state or reflect those of the United States Government or any agency thereof.

Biographies

Kevin Pastoor is currently a graduate student at the Colorado School of Mines. His research is focused on uranium chemistry related to the nuclear fuel cycle and nuclear security.

R. Scott Kemp is currently the MIT Class of '43 Associate Professor of Nuclear Science and Engineering and director of the MIT Laboratory for Nuclear Security and Policy. His research combines physics, politics, and history to help create more resilient societies. His work has focused primarily on problems arising from weapons of mass destruction and energy.

https://doi.org/10.1021/acs.inorgchem.0c03390
Inorg. Chem. XXXX, XXX, XXX−XXX

Mark Jensen is currently a Professor, Department of Chemistry, and the Jerry and Tina Grandey University Chair in Nuclear Science and Engineering at the Colorado School of Mines. His research is focused on the nuclear fuel cycle, ranging from mechanisms of selectivity in chemical separations to biologically based metal separations and the biochemistry and environmental chemistry of the transuranium elements.

Jenifer Shafer is currently an Associate Professor, Department of Chemistry, at the Colorado School of Mines. She conducts chemical research related to nuclear energy and security.

■ ACKNOWLEDGMENTS

J.C.S. and K.J.P. acknowledge support from the Department of Energy/National Nuclear Security Administration under Award DE-NA0003921. M.P.J. acknowledges support from the Colorado School of Mines. The views and conclusions expressed in this document are those of the authors and do not reflect the official policy or position of the United States Air Force, Department of Defense, or the U.S. Government.

■ REFERENCES

(1) Tsoulfanidis, N. Review of the Nuclear Fuel Cycle. In *The Nuclear Fuel Cycle*; American Nuclear Society: La Grange Park, IL, 2013; pp 1−26.
(2) *Nuclear Forensics in Support of Investigations*; IAEA: Vienna, Austria, 2015; pp 1−62.
(3) Keegan, E.; Kristo, M. J.; Toole, K.; Kips, R.; Young, E. Nuclear Forensics: Scientific Analysis Supporting Law Enforcement and Nuclear Security Investigations. *Anal. Chem.* **2016**, *88*, 1496−1505.
(4) Mayer, K. Expand Nuclear Forensics. *Nature* **2013**, *503*, 461−462.
(5) Mayer, K.; Wallenius, M.; Varga, Z. Nuclear Forensic Science: Correlating Measurable Material Parameters to the History of Nuclear Material. *Chem. Rev.* **2013**, *113*, 884−900.
(6) Moody, K. J.; Hutcheon, I. D.; Grant, P. M. *Nuclear Forensic Analysis*, 2nd ed.; CRC Press: Boca Raton, FL, 2015; p 502.
(7) Hutcheon, I.; Kristo, M.; Knight, K. *Nonproliferation Nuclear Forensics, LLNL-CONF-679869*; Lawrence Livermore National Laboratory, CA, 2015; pp 1−18.
(8) May, M.; Abedin-Zadeh, R.; Barr, D.; Carnesale, A.; Coyle, P. E.; Davis, J.; Dorland, W.; Dunlop, W.; Fetter, S.; Glaser, A.; Hutcheon, I. D.; Slakey, F.; Tannebaum, B. *Nuclear Forensics: Role, State of the Art, and Program Needs*; American Association for the Advancement of Science and the American Physical Society: Washington, DC, 2008; pp 1−59.
(9) Kemp, R. S. Environmental Detection of Clandestine Nuclear Weapon Programs. *Annu. Rev. Earth Planet. Sci.* **2016**, *44*, 17−35.
(10) Hastings, J. V.; Vestergaard, C. Safeguards and Security Risks at the (Very) Front End of the Nuclear Fuel Cycle. *Nonproliferation Review* **2018**, *25*, 457−476.
(11) The Mineralogy of Uranium. https://www.mindat.org/element/Uranium (accessed June 15, 2020).
(12) Krivovichev, V. G.; Charykova, M. V. Number of Minerals of Various Chemical Elements: Statistics 2012 (a new approach to an old problem). *Geol. Ore Deposits* **2014**, *56*, 553−559.
(13) Tsoulfanidis, N. Nuclear Fuel Resources, Mining, and Milling. In *The Nuclear Fuel Cycle*; American Nuclear Society: La Grange Park, IL, 2013; pp 28−56.
(14) Woods, P. H. Uranium Mining (Open Cut and Underground) and Milling. In *Uranium for Nuclear Power*; Hore-Lacy, I., Ed.; Woodhead Publishing, 2016; pp 125−156.
(15) Oliver, A. J.; Özberk, E. Conversion of Natural Uranium. In *Uranium for Nuclear Power*; Hore-Lacy, I., Ed.; Woodhead Publishing, 2016; pp 299−319.
(16) Tsoulfanidis, N. Conversion and Enrichment. In *The Nuclear Fuel Cycle*; American Nuclear Society: La Grange Park, IL, 2013; pp 57−85.
(17) Harding, P. Uranium Enrichment. In *Uranium for Nuclear Power*; Hore-Lacy, I., Ed.; Woodhead Publishing, 2016; pp 321−351.
(18) Supko, E. Nuclear Fuel Fabrication. In *Uranium for Nuclear Power*; Hore-Lacy, I., Ed.; Woodhead Publishing, 2016; pp 353−382.
(19) Tsoulfanidis, N. Reactor Fuel Design and Fabrication. In *The Nuclear Fuel Cycle*; American Nuclear Society: La Grange Park, IL, 2013; pp 86−119.
(20) Abbott, E. C.; Brenkmann, A.; Galbraith, C.; Ong, J.; Schwerdt, I. J.; Albrecht, B. D.; Tasdizen, T.; McDonald, L. W. Dependence of UO_2 Surface Morphology on Processing History within a Single Synthetic Route. *Radiochim. Acta* **2019**, *107*, 1121−1131.
(21) Hanson, A. B.; Lee, R. N.; Vachet, C.; Schwerdt, I. J.; Tasdizen, T.; McDonald, L. W. Quantifying Impurity Effects on the Surface Morphology of α-U_3O_8. *Anal. Chem.* **2019**, *91*, 10081−10087.
(22) Heffernan, S. T.; Ly, N. C.; Mower, B. J.; Vachet, C.; Schwerdt, I. J.; Tasdizen, T.; McDonald, L. W. Identifying Surface Morphological Characteristics to Differentiate Between Mixtures of U_3O_8 Synthesized from Ammonium Diuranate and Uranyl Peroxide. *Radiochim. Acta* **2020**, *108*, 29−36.
(23) Ly, C.; Olsen, A. M.; Schwerdt, I. J.; Porter, R.; Sentz, K.; McDonald, L. W.; Tasdizen, T. A New Approach for Quantifying Morphological Features of U_3O_8 for Nuclear Forensics Using a Deep Learning Model. *J. Nucl. Mater.* **2019**, *517*, 128−137.
(24) Ly, C.; Vachet, C.; Schwerdt, I.; Abbott, E.; Brenkmann, A.; McDonald, L. W.; Tasdizen, T. Determining Uranium Ore Concentrates and their Calcination Products via Image Classification of Multiple Magnifications. *J. Nucl. Mater.* **2020**, *533*, 152082.
(25) Olsen, A. M.; Richards, B.; Schwerdt, I.; Heffernan, S.; Lusk, R.; Smith, B.; Jurrus, E.; Ruggiero, C.; McDonald, L. W. Quantifying Morphological Features of α-U_3O_8 with Image Analysis for Nuclear Forensics. *Anal. Chem.* **2017**, *89*, 3177−3183.
(26) Olsen, A. M.; Schwerdt, I.; Jolley, A.; Halverson, N.; Richards, B.; McDonald, L. W. A Response Surface Model of Morphological Changes in UO_2 and U_3O_8 Following High Temperature Aging. *Radiochim. Acta* **2019**, *107*, 449−458.

https://doi.org/10.1021/acs.inorgchem.0c03390
Inorg. Chem. XXXX, XXX, XXX−XXX

(27) Schwerdt, I. J.; Hawkins, C. G.; Taylor, B.; Brenkmann, A.; Martinson, S.; McDonald, L. W. Uranium Oxide Synthetic Pathway Discernment Through Thermal Decomposition and Morphological Analysis. *Radiochim. Acta* **2019**, *107*, 193−205.
(28) Schwerdt, I. J.; Olsen, A.; Lusk, R.; Heffernan, S.; Klosterman, M.; Collins, B.; Martinson, S.; Kirkham, T.; McDonald, L. W. Nuclear Forensics Investigation of Morphological Signatures in the Thermal Decomposition of Uranyl Peroxide. *Talanta* **2018**, *176*, 284−292.
(29) Tamasi, A. L.; Cash, L. J.; Mullen, W. T.; Pugmire, A. L.; Ross, A. R.; Ruggiero, C. E.; Scott, B. L.; Wagner, G. L.; Walensky, J. R.; Wilkerson, M. P. Morphology of U_3O_8 Materials Following Storage Under Controlled Conditions of Temperature and Relative Humidity. *J. Radioanal. Nucl. Chem.* **2017**, *311*, 35−42.
(30) Tamasi, A. L.; Cash, L. J.; Mullen, W. T.; Ross, A. R.; Ruggiero, C. E.; Scott, B. L.; Wagner, G. L.; Walensky, J. R.; Zerkle, S. A.; Wilkerson, M. P. Comparison of Morphologies of a Uranyl Peroxide Precursor and Calcination Products. *J. Radioanal. Nucl. Chem.* **2016**, *309*, 827−832.
(31) Manna, S.; Karthik, P.; Mukherjee, A.; Banerjee, J.; Roy, S. B.; Joshi, J. B. Study of Calcinations of Ammonium Diuranate at Different Temperatures. *J. Nucl. Mater.* **2012**, *426*, 229−232.
(32) Manna, S.; Roy, S. B.; Joshi, J. B. Study of Crystallization and Morphology of Ammonium Diuranate and Uranium Oxide. *J. Nucl. Mater.* **2012**, *424*, 94−100.
(33) Tamasi, A. L.; Cash, L. J.; Eley, C.; Porter, R. B.; Pugmire, D. L.; Ross, A. R.; Ruggiero, C. E.; Tandon, L.; Wagner, G. L.; Walensky, J. R.; Wall, A. D.; Wilkerson, M. P. A Lexicon for Consistent Description of Material Images for Nuclear Forensics. *J. Radioanal. Nucl. Chem.* **2016**, *307*, 1611−1619.
(34) Balboni, E.; Jones, N.; Spano, T.; Simonetti, A.; Burns, P. C. Chemical and Sr Isotopic Characterization of North America Uranium Ores: Nuclear Forensic Applications. *Appl. Geochem.* **2016**, *74*, 24−32.
(35) Balboni, E.; Simonetti, A.; Spano, T.; Cook, N. D.; Burns, P. C. Rare-earth Element Fractionation in Uranium Ore and its U(VI) Alteration Minerals. *Appl. Geochem.* **2017**, *87*, 84−92.
(36) Fahey, A. J.; Ritchie, N. W. M.; Newbury, D. E.; Small, J. A. The Use of Lead Isotopic Abundances in Trace Uranium Samples for Nuclear Forensics Analysis. *J. Radioanal. Nucl. Chem.* **2010**, *284*, 575−581.
(37) Spano, T. L.; Simonetti, A.; Balboni, E.; Dorais, C.; Burns, P. C. Trace Element and U Isotope Analysis of Uraninite and Ore Concentrate: Applications for Nuclear Forensic Investigations. *Appl. Geochem.* **2017**, *84*, 277−285.
(38) Spano, T. L.; Simonetti, A.; Wheeler, T.; Carpenter, G.; Freet, D.; Balboni, E.; Dorais, C.; Burns, P. C. A Novel Nuclear Forensic Tool Involving Deposit Type Normalized Rare Earth Element Signatures. *Terra Nova* **2017**, *29*, 294−305.
(39) Svedkauskaite-LeGore, J.; Mayer, K.; Millet, S.; Nicholl, A.; Rasmussen, G.; Baltrunas, D. Investigation of the Isotopic Composition of Lead and of Trace Elements Concentrations in Natural Uranium Materials as a Signature in Nuclear Forensics. *Radiochim. Acta* **2007**, *95*, 601−605.
(40) Varga, Z.; Krajko, J.; Penkin, M.; Novak, M.; Eke, Z.; Wallenius, M.; Mayer, K. Identification of Uranium Signatures Relevant for Nuclear Safeguards and Forensics. *J. Radioanal. Nucl. Chem.* **2017**, *312*, 639−654.
(41) Varga, Z.; Wallenius, M.; Mayer, K. Origin Assessment of Uranium Ore Concentrates Based on their Rare-earth Elemental Impurity Pattern. *Radiochim. Acta* **2010**, *98*, 771−778.
(42) Varga, Z.; Wallenius, M.; Mayer, K.; Keegan, E.; Millet, S. Application of Lead and Strontium Isotope Ratio Measurements for the Origin Assessment of Uranium Ore Concentrates. *Anal. Chem.* **2009**, *81*, 8327−8334.
(43) Kristo, M. J.; Tumey, S. J. The state of nuclear forensics. *Nucl. Instrum. Methods Phys. Res., Sect. B* **2013**, *294*, 656−661.
(44) Keegan, E.; Wallenius, M.; Mayer, K.; Varga, Z.; Rasmussen, G. Attribution of Uranium Ore Concentrates Using Elemental and Anionic Data. *Appl. Geochem.* **2012**, *27*, 1600−1609.
(45) Badaut, V.; Wallenius, M.; Mayer, K. Anion Analysis in Uranium Ore Concentrates by Ion Chromatography. *J. Radioanal. Nucl. Chem.* **2009**, *280*, 57−61.
(46) Nizinski, C. A.; Hanson, A. B.; Fullmer, B. C.; Mecham, N. J.; Tasdizen, T.; McDonald, L. W. Effects of Process History on the Surface Morphology of Uranium Ore Concentrates Extracted from Ore. *Miner. Eng.* **2020**, *156*, 106457.
(47) Shollenberger, Q. R.; Borg, L. E.; Ramon, E. C.; Sharp, M. A.; Brennecka, G. A. Samarium Isotope Compositions of Uranium Ore Concentrates: A Novel Nuclear Forensic Signature. *Talanta* **2021**, *221*, 121431.
(48) Rolison, J. M.; Druce, M.; Shollenberger, Q. R.; Kayzar-Boggs, T. M.; Lindvall, R. E.; Wimpenny, J. Molybdenum Isotope Compositions of Uranium Ore Concentrates by Double Spike MC-ICP-MS. *Appl. Geochem.* **2019**, *103*, 97−105.
(49) Migeon, V.; Fitoussi, C.; Pili, E.; Bourdon, B. Molybdenum Isotope Fractionation in Uranium Oxides and During Key Processes of the Nuclear Fuel Cycle: Towards a New Nuclear Forensic Tool. *Geochim. Cosmochim. Acta* **2020**, *279*, 238−257.
(50) Krajko, J.; Varga, Z.; Yalcintas, E.; Wallenius, M.; Mayer, K. Application of Neodymium Isotope Ratio Measurements for the Origin Assessment of Uranium Ore Concentrates. *Talanta* **2014**, *129*, 499−504.
(51) Donald, S. B.; Dai, Z. R. R.; Davisson, M. L.; Jeffries, J. R.; Nelson, A. J. An XPS Study on the Impact of Relative Humidity on the Aging of UO_2 Powders. *J. Nucl. Mater.* **2017**, *487*, 105−112.
(52) Guo, X.; Ushakov, S. V.; Labs, S.; Curtius, H.; Bosbach, D.; Navrotsky, A. Energetics of Metastudtite and Implications for Nuclear Waste Alteration. *Proc. Natl. Acad. Sci. U. S. A.* **2014**, *111*, 17737−17742.
(53) Guo, X.; Wu, D.; Ushakov, S. V.; Shvareva, T.; Xu, H.; Navrotsky, A. Energetics of Hydration on Uranium Oxide and Peroxide Surfaces. *J. Mater. Res.* **2019**, *34*, 3319−3325.
(54) Guo, X.; Wu, D.; Xu, H. W.; Burns, P. C.; Navrotsky, A. Thermodynamic Studies of Studtite Thermal Decomposition Pathways via Amorphous Intermediates UO_3, U_2O_7, and UO_4. *J. Nucl. Mater.* **2016**, *478*, 158−163.
(55) Odoh, S. O.; Shamblin, J.; Colla, C. A.; Hickam, S.; Lobeck, H. L.; Lopez, R. A. K.; Olds, T.; Szymanowski, J. E. S.; Sigmon, G. E.; Neuefeind, J.; Casey, W. H.; Lang, M.; Gagliardi, L.; Burns, P. C. Structure and Reactivity of X-ray Amorphous Uranyl Peroxide, U_2O_7. *Inorg. Chem.* **2016**, *55*, 3541−3546.
(56) Tamasi, A. L.; Boland, K. S.; Czerwinski, K.; Ellis, J. K.; Kozimor, S. A.; Martin, R. L.; Pugmire, A. L.; Reilly, D.; Scott, B. L.; Sutton, A. D.; Wagner, G. L.; Walensky, J. R.; Wilkerson, M. P. Oxidation and Hydration of U_3O_8 Materials Following Controlled Exposure to Temperature and Humidity. *Anal. Chem.* **2015**, *87*, 4210−4217.
(57) Tracy, C. L.; Chen, C. H.; Park, S.; Davisson, M. L.; Ewing, R. C. Measurement of UO_2 Surface Oxidation Using Grazing-incidence X-ray Diffraction: Implications for Nuclear Forensics. *J. Nucl. Mater.* **2018**, *502*, 68−75.
(58) Wilkerson, M. P.; Hernandez, S. C.; Mullen, W. T.; Nelson, A. T.; Pugmire, A. L.; Scott, B. L.; Sooby, E. S.; Tamasi, A. L.; Wagner, G. L.; Walensky, J. R. Hydration of α-UO_3 Following Storage Under Controlled Conditions of Temperature and Relative Humidity. *Dalton Transactions* **2020**, *49*, 10452−10462.
(59) Tobin, J. G.; Duffin, A. M.; Yu, S. W.; Qiao, R.; Yang, W. L.; Booth, C. H.; Shuh, D. K. Surface Degradation of Uranium Tetrafluoride. *J. Vac. Sci. Technol., A* **2017**, *35*, 03E108.
(60) Wellons, M.; DeVore, M.; Villa-Aleman, E.; Summer, M.; Smith, R.; Klug, C.; Daroudi, T. *Characterization of the Environmentally Induced Chemical Transformations of Uranium Tetrafluoride, SRNL-MS-2017-00048*; Savannah River National Laboratory: Aiken, SC, 2017; pp 101−106.
(61) Kips, R.; Crowhurst, J.; Kristo, M. J.; Stefaniak, E.; Hutcheon, I. D. *Micro-Raman Spectroscopy of Uranium Oxyfluoride Particulate Material for Nuclear Safeguards, LLNL-PROC-433314*; Lawrence Livermore National Laboratory: Livermore, CA, 2010; pp 1−10.

https://doi.org/10.1021/acs.inorgchem.0c03390
Inorg. Chem. XXXX, XXX, XXX−XXX

(62) Kips, R.; Kristo, M. J.; Crowhurst, J.; Hutcheon, I. D.; Stefaniak, E.; Aregbe, Y. *Investigating Chemical and Molecular Changes in Uranium Oxyfluoride Particles using NanoSIMS and Micro-Raman Spectroscopy, LLNL-PROC-455709*; Lawrence Livermore National Laboratory: Livermore, CA, 2010; pp 1−9.
(63) Kips, R.; Leenaers, A.; Tamborini, G.; Betti, M.; Van den Berghe, S.; Wellum, R.; Taylor, P. Characterization of Uranium Particles Produced by Hydrolysis of UF_6 Using SEM and SIMS. *Microsc. Microanal.* **2007**, *13*, 156−164.
(64) Kips, R.; Pidduck, A. J.; Houlton, M. R.; Leenaers, A.; Mace, J. D.; Marie, O.; Pointurier, F.; Stefaniak, E. A.; Taylor, P. D. P.; Van den Berghe, S.; Van Espen, P.; Van Grieken, R.; Wellum, R. Determination of Fluorine in Uranium Oxyfluoride Particles as an Indicator of Particle Age. *Spectrochim. Acta, Part B* **2009**, *64*, 199−207.
(65) Kips, R. S.; Kristo, M. J. Investigation of Chemical Changes in Uranium Oxyfluoride Particles Using Secondary Ion Mass Spectrometry. *J. Radioanal. Nucl. Chem.* **2009**, *282*, 1031−1035.
(66) Kirkegaard, M. C.; Ambrogio, M. W.; Miskowiec, A.; Shields, A. E.; Niedziela, J. L.; Spano, T. L.; Anderson, B. B. Characterizing the Degradation of $[(UO_2F_2)(H_2O)]_7{\cdot}4H_2O$ Under Humid Conditions. *J. Nucl. Mater.* **2020**, *529*, 151889.
(67) Kirkegaard, M. C.; Miskowiec, A.; Ambrogio, M. W.; Anderson, B. B. Evidence of a Nonphotochemical Mechanism for the Solid-State Formation of Uranyl Peroxide. *Inorg. Chem.* **2018**, *57*, 5711−5715.
(68) Kirkegaard, M. C.; Spano, T. L.; Ambrogio, M. W.; Niedziela, J. L.; Miskowiec, A.; Shields, A. E.; Anderson, B. B. Formation of a Uranyl Hydroxide Hydrate via Hydration of $[(UO_2F_2)(H_2O)]_7{\cdot}4H_2O$. *Dalton Transactions* **2019**, *48*, 13685−13698.
(69) Pointurier, F.; Lelong, C.; Marie, O. Study of the Chemical Changes of μm-Sized Particles of Uranium Tetrafluoride (UF_4) in Environmental Conditions by Means of micro-Raman Spectrometry. *Vib. Spectrosc.* **2020**, *110*, 103145.
(70) Campbell, K. R.; Wozniak, N. R.; Colgan, J. P.; Judge, E. J.; Barefield, J. E.; Kilcrease, D. P.; Wilkerson, M. P.; Czerwinski, K. R.; Clegg, S. M. Phase Discrimination of Uranium Oxides Using Laser-induced Breakdown Spectroscopy. *Spectrochim. Acta, Part B* **2017**, *134*, 91−97.
(71) He, H. M.; Wang, P.; Allred, D. D.; Majewski, J.; Wilkerson, M. P.; Rector, K. D. Characterization of Chemical Speciation in Ultrathin Uranium Oxide Layered Films. *Anal. Chem.* **2012**, *84*, 10380−10387.
(72) Ho, D. M. L.; Jones, A. E.; Goulermas, J. Y.; Turner, P.; Varga, Z.; Fongaro, L.; Fanghanel, T.; Mayer, K. Raman Spectroscopy of Uranium Compounds and the Use of Multivariate Analysis for Visualization and Classification. *Forensic Sci. Int.* **2015**, *251*, 61−68.
(73) Pointurier, F.; Marie, O. Identification of the Chemical Forms of Uranium Compounds in Micrometer-size Particles by Means of Micro-Raman Spectrometry and Scanning Electron Microscope. *Spectrochim. Acta, Part B* **2010**, *65*, 797−804.
(74) Shattan, M. B.; Miller, D. J.; Cook, M. T.; Stowe, A. C.; Auxier, J. D.; Parigger, C.; Hall, H. L. Detection of Uranyl Fluoride and Sand Surface Contamination on Metal Substrates by Hand-held Laser-induced Breakdown Spectroscopy. *Appl. Opt.* **2017**, *56*, 9868−9875.
(75) Skrodzki, P. J.; Burger, M.; Finney, L. A.; Poineau, F.; Balasekaran, S. M.; Nees, J.; Czerwinski, K. R.; Jovanovic, I. Ultrafast Laser Filament-induced Fluorescence Spectroscopy of Uranyl Fluoride. *Sci. Rep.* **2018**, *8*, 11629.
(76) Ward, J. D.; Bowden, M.; Tom Resch, C.; Eiden, G. C.; Pemmaraju, C. D.; Prendergast, D.; Duffin, A. M. Identifying Anthropogenic Uranium Compounds Using Soft X-ray Near-edge Absorption Spectroscopy. *Spectrochim. Acta, Part B* **2017**, *127*, 20−27.
(77) Schwerdt, I. J.; Brenkmann, A.; Martinson, S.; Albrecht, B. D.; Heffernan, S.; Klosterman, M. R.; Kirkham, T.; Tasdizen, T.; McDonald, L. W. Nuclear Proliferomics: A New Field of Study to Identify Signatures of Nuclear Materials as Demonstrated on α-UO_3. *Talanta* **2018**, *186*, 433−444.
(78) Burns, P. C.; Hughes, K. A. Studtite, $[(UO_2)(O_2)(H_2O)_2]$-$(H_2O)_2$: The First Structure of a Peroxide Mineral. *Am. Mineral.* **2003**, *88*, 1165−1168.
(79) Kubatko, K. A. H.; Helean, K. B.; Navrotsky, A.; Burns, P. C. Stability of Peroxide-Containing Uranyl Minerals. *Science* **2003**, *302*, 1191−1193.
(80) Kuhn, E.; Fischer, D.; Ryjinski, M. *Environmental Sampling for IAEA Safeguards: A Five Year Review, IAEA-SM-367/10/01*; IAEA: Vienna, Austria, 2001; pp 1−7.
(81) *Standard Specification for Uranium Hexafluoride for Enrichment; C0787-20*; ASTM International: West Conshohocken, PA, 2020.
(82) *Standard Test Methods for Chemical, Mass Spectrometric, Spectrochemical, Nuclear, and Radiochemical Analysis of Uranium Hexafluoride; C0761-18*; ASTM International: West Conshohocken, PA, 2018.
(83) Van Veen, E. H.; Deloosvollebregt, M. T. C.; Wassink, A. P.; Kalter, H. Determination of Trace-Elements in Uranium by Inductively Coupled Plasma-Atomic Emission-Spectrometry Using Kalman Filtering. *Anal. Chem.* **1992**, *64*, 1643−1649.
(84) Reilly, D. D.; Athon, M. T.; Corbey, J. E.; Leavy, I. I.; McCoy, K. M.; Schwantes, J. M. Trace Element Migration During UF_4 Bomb Reduction: Implications to Metal Fuel Production, Worker Health and Safety, and Nuclear Forensics. *J. Nucl. Mater.* **2018**, *510*, 156−162.
(85) Stanley, F. E. A Beginner's Guide to Uranium Chronometry in Nuclear Forensics and Safeguards. *J. Anal. At. Spectrom.* **2012**, *27*, 1821−1830.
(86) Katz, J. J.; Rabinowitch, E. Nonvolatile Fluorides of Uranium. In *The Chemistry of Uranium: The Element, its Binary and Related Compounds*; Dover Publications, Inc., New York, 1961; pp 349−395.
(87) Domange, L.; Wohlhuter, M. Sensibilite Du Fluorure Duranium F_4U a La Vapeur Deau. *Compt. Rend.* **1949**, *228*, 1591−1592.
(88) Warf, J. C.; Cline, W. D.; Tevebaugh, R. D. Pyrohydrolysis in the Determination of Fluoride and Other Halides. *Anal. Chem.* **1954**, *26*, 342−346.
(89) Hibbits, J. O. Precision of the Pyrohydrolytic Determination of Fluoride and Uranium in Uranyl Fluoride and Uranium Tetrafluoride. *Anal. Chem.* **1957**, *29*, 1760−1762.
(90) Iwasaki, M.; Ishikawa, N. Pyrohydrolysis Reactions of UF_4 and UO_2F_2 - Effect of Oxygen on Reactions. *J. Nucl. Sci. Technol.* **1983**, *20*, 400−404.
(91) Cong, P. J.; Cao, S.; Sun, H.; Tan, X.; Wang, R. S. Determination of Fluorine in UF_4 by High-temperature Hydrolysis. *J. Radioanal. Nucl. Chem.* **1999**, *242*, 811−814.
(92) Dong, X. Y.; Zheng, X. B.; Song, Y. L.; Liu, Y. X.; Zhang, L. Pyrohydrolysis of Uranium Tetrafluoride and Thorium Tetrafluoride. *He Huaxue Yu Fangshe Huaxue* **2014**, *36*, 181−185.
(93) Zhong, J. R.; Shao, L.; Yu, C. R.; Ren, Y. M. Study of Thermal Chemical Reaction of UF_4 in Air, O_2, and Hydrated O_2. *Acta Physico-Chimica Sinica* **2015**, *31*, 25−31.
(94) Grenthe, I.; Drożdżyński, J.; Fujino, T.; Buck, E. C.; Albrecht-Schmitt, T. E.; Wolf, S. F. Uranium. In *The Chemistry of the Actinide and Transactinide Elements*; Morss, L. R., Edelstein, N. M., Fuger, J., Eds.; Springer: Dordrecht, The Netherlands, 2010; pp 253−698.
(95) Grosse, A. V. *Chemical Properties of Uranium Hexafluoride, UF_6, A-83*; Columbia University: New York, 1941.
(96) Ruff, O.; Heinzelmann, A. On Uranium Hexaflouride. *Z. Anorg. Chem.* **1911**, *72*, 63−84.
(97) Sherrow, S. A.; Hunt, R. D. FTIR Spectra of the Hydrolysis of Uranium Hexafluoride. *J. Phys. Chem.* **1992**, *96*, 1095−1099.
(98) Richards, J. M.; Martin, L. R.; Fugate, G. A.; Cheng, M. D. Kinetic Investigation of the Hydrolysis of Uranium Hexafluoride Gas. *RSC Adv.* **2020**, *10*, 34729−34731.
(99) Wagner, G. L.; Kinkead, S. A.; Paffett, M. T.; Rector, K. D.; Scott, B. L.; Tamasi, A. L.; Wilkerson, M. P. Morphologic and Chemical Characterization of Products from Hydrolysis of UF_6. *J. Fluorine Chem.* **2015**, *178*, 107−114.
(100) Hu, S. W.; Lin, H.; Wang, X. Y.; Chu, T. W. Effect of H_2O on the Hydrolysis of UF_6 in the Gas Phase. *J. Mol. Struct.* **2014**, *1062*, 29−34.

https://doi.org/10.1021/acs.inorgchem.0c03390
Inorg. Chem. XXXX, XXX, XXX−XXX

(101) Hu, S. W.; Wang, X. Y.; Chu, T. W.; Liu, X. Q. Theoretical Mechanism Study of UF_6 Hydrolysis in the Gas Phase. *J. Phys. Chem. A* **2008**, *112*, 8877−8883.
(102) Hu, S. W.; Wang, X. Y.; Chu, T. W.; Liu, X. Q. Theoretical Mechanism Study of UF_6 Hydrolysis in the Gas Phase (II). *J. Phys. Chem. A* **2009**, *113*, 9243−9248.
(103) Klimov, V. D.; Kravetz, Y. M.; Besmelnitzin, A. V. Investigation of Uranium Hexafluoride Hydrolysis Kinetics by Laser HF Analyzer. *J. Fluorine Chem.* **1992**, *58*, 262.
(104) Bostick, W. D.; Mcculla, W. H.; Pickrell, P. W. Sampling, Characterization, and Remote-Sensing of Aerosols Formed in the Atmospheric Hydrolysis of Uranium Hexafluoride. *J. Environ. Sci. Health, Part A: Environ. Sci. Eng.* **1985**, *20*, 369−393.
(105) Armstrong, D. P.; Bostick, W. D.; Fletcher, W. H. An FT-IR Study of the Atmospheric Hydrolysis of Uranium Hexafluoride. *Appl. Spectrosc.* **1991**, *45*, 1008−1016.
(106) Pickrell, P. W. *Characterization of the Solid, Airborne Materials Created by the Interaction of UF_6 with Atmospheric Moisture in a Contained Vol., K/PS-144*; Oak Ridge Gaseous Diffusion Plant: Oak Ridge, TN, 1982; pp 1−89.
(107) Lux, C. J. *Evaluation of Techniques for Controlling UF_6 Release Clouds in the GAT Environmental Chamber, GAT-T-3116*; Goodyear Atomic Corp.: Piketon, OH, 1982; pp 1−22.
(108) Cheng, M.-D.; Richards, J. M.; Omana, M. A.; Hubbard, J. A.; Fugate, G. A. Experimental and Computational Study of Particle Formation Kinetics in UF_6 Hydrolysis. *React. Chem. Eng.* **2020**, *5*, 1708−1718.
(109) Kemp, R. S. Initial Analysis of the Detectability of UO_2F_2 Aerosols Produced by UF_6 Released from Uranium Conversion Plants. *Science & Global Security* **2008**, *16*, 115−125.
(110) Bullock, J. I. Raman and Infrared Spectroscopic Studies of Uranyl Ion - Symmetric Stretching Frequency Force Constants and Bond Lengths. *J. Chem. Soc. A* **1969**, 781−784.
(111) Stefaniak, E. A.; Darchuk, L.; Sapundjiev, D.; Kips, R.; Aregbe, Y.; Van Grieken, R. New Insight into UO_2F_2 Particulate Structure by Micro-Raman Spectroscopy. *J. Mol. Struct.* **2013**, *1040*, 206−212.
(112) Kips, R.; Kristo, M. J.; Hutcheon, I. D.; Amonette, J.; Wang, Z.; Johnson, T.; Gerlach, D.; Olsen, K. B. *Determination of the Relative Amount of Fluorine in Uranium Oxyfluoride Particles using Secondary Ion Mass Spectrometry and Optical Spectroscopy, LLNL-PROC-414029*; Lawrence Livermore National Laboratory: Livermore, CA, 2009; pp 1−10.
(113) Beitz, J. V.; Williams, C. W. Uranyl Fluoride Luminescence in Acidic Aqueous Solutions. *J. Alloys Compd.* **1997**, *250*, 375−379.
(114) Su, J.; Wang, Z. M.; Pan, D. Q.; Li, J. Excited States and Luminescent Properties of UO_2F_2 and Its Solvated Complexes in Aqueous Solution. *Inorg. Chem.* **2014**, *53*, 7340−7350.
(115) Katz, J. J.; Rabinowitch, E. Uranium Oxyhalides. In *The Chemistry of Uranium: The Element, its Binary and Related Compounds*; Dover Publications, Inc., New York, 1961; pp 564−599.
(116) Ferris, L. M.; Baird, F. G. Decomposition of Uranyl Fluoride between 700°C and 950°C. *J. Electrochem. Soc.* **1960**, *107*, 305−308.
(117) Knacke, O.; Lossmann, G.; Muller, F. Thermal Dissociation and Sublimation of UO_2F_2. *Z. Anorg. Allg. Chem.* **1969**, *371*, 32−37.
(118) Lau, K. H.; Brittain, R. D.; Hildenbrand, D. L. Complex Sublimation/Decomposition of Uranyl Fluoride: Thermodynamics of Gaseous UO_2F_2 and UOF_4. *J. Phys. Chem.* **1985**, *89*, 4369−4373.
(119) Wang, Y. H.; von Gunten, K.; Bartova, B.; Meisser, N.; Astner, M.; Burger, M.; Bernier-Latmani, R. Products of in Situ Corrosion of Depleted Uranium Ammunition in Bosnia and Herzegovina Soils. *Environ. Sci. Technol.* **2016**, *50*, 12266−12274.

https://doi.org/10.1021/acs.inorgchem.0c03390
Inorg. Chem. XXXX, XXX, XXX−XXX